

Surface enhanced Raman spectroscopy (SERS) based detection schemes for food analytics



seit 1558

Friedrich-Schiller-Universität Jena

Dissertation

zur Erlangung des akademischen Grades doctor rerum naturalium
(Dr. rer. nat.)

vorgelegt dem Rat der Chemisch-Geowissenschaftliche Fakultät der
Friedrich-Schiller-Universität Jena

von M.Sc. Andreea – Ioana Radu
geboren am 06.02.1987 in Turda, Rumänien

Gutachter:

1. Prof. Dr. Jürgen Popp

(Institut für Physikalische Chemie, Friedrich-Schiller-Universität Jena)

2. Prof. Dr. Volker Deckert

(Institut für Physikalische Chemie, Friedrich-Schiller-Universität Jena)

Tag der Verteidigung: 8. Juli 2016

Table of Contents

Abbreviations	III
Introduction	1
Einleitung	3
1. Basics	5
1.1. Why to analyze food?	5
1.1.1. Vitamins B2 and B12 and their dietary importance	7
1.1.2. Dietary benefits of β -car and lyc.....	8
1.2. State of the art in food analytics	9
1.2.1. HPLC	9
1.2.2. Microbiological assay	12
1.3 SERS – an emerging technique for the field of food analytics	12
1.3.1. Requirements for performing SERS measurements	14
1.3.2. The best-suited SERS-active substrate for food analytics	15
1.3.3. Chemometric-based tools for fast food analysis.....	18
2. Materials and methods	19
2.1. Chemicals and reagents	19
2.2. SERS active substrates	20
2.3. Sample preparation.....	23
2.4. Food extraction.....	26
2.5. HPLC measurements	27
2.6. Spectroscopic measurements.....	28
2.7. Chemometric-based analysis	30
3. Results and discussion.....	32
3.1. Characterization of SERS-active substrates as powerful platform for food analytics	32

3.1.1. Enzymatically generated silver nanoparticles (EGNPs)	34
3.1.2. Nano-sponges (NSs)	38
3.1.3. HD-DVD-based substrates.....	42
3.1.4. EBL-based substrates	48
3.2. SERS-based applications for food analytics.....	54
3.2.1. The detection and differentiation of two B vitamins in simulated and market available fortified cereal product	54
3.2.2. The estimation of the amount of two carotenoids in tomatoes	65
4. Summary and outlook	76
5. References	80
Curriculum vitae.....	V
Acknowledgment.....	VIII
Declaration of Originality	X

Abbreviations

Ag	silver
Au	gold
Ag/Au NSs	Ag/Au nanosponges
ALD	atomic layer deposition
B1	thiamine (vitamin B1)
B2	riboflavin (vitamin B2)
B3	niacin (vitamin B3)
B5	pantothenic acid (vitamin B5)
B6	pyridoxine, pyridoxal, pyridoxamine (vitamin B6)
B7	biotin (vitamin B7)
B9	folic acid (vitamin B9)
B12	cyanocobalamin (vitamin B12)
BCMO1	enzyme β -car-monooxygenase-1
β -car	β -car
BY	butter yellow
BSFM	B vitamin simulated food matrix
CE	cereal extract
EBL	electron beam lithography
EGNPs	enzymatically generated silver nanoparticles
EFSA	European food safety authority
F	fructose
FEM	finite-element modelling
G	glucose
HPLC	high performance liquid chromatography
HRP	streptavidin horseradish peroxidase
HQ	hydroquinone
ICP	inductively coupled plasma

LoD	limit of detection
LoQ	limit of quantification
lyc	lyc
LSPP	localized surface plasmon polaritons
LR-SPP	long-range surface plasmon polaritons
MS	mass spectrometry
MeOH	methanol
NSs	“nanosponge-like” substrates
PCA	principal component analysis
PLSR	partial least squares regression
PBS	phosphate buffered saline
PC	polycarbonate
PICT	photon-induced charge-transfer
PSPP	propagating surface plasmon polaritons
RSD	relative standard deviation
RMSE	root mean square error
ROS	reactive oxygen species
S	sucrose
SNIP	sensitive nonlinear iterative peak
SERS	surface enhanced Raman spectroscopy
SERRS	surface enhanced resonant Raman spectroscopy
SEM	scanning electron microscopy
SR-SPP	short-range surface plasmon polaritons
SPE	solid phase extractions
SPs	surface plasmons
SPR	surface plasmon resonance
tBME	tertiary butyl methyl ether
USFDA	U.S. food and drug administration

Introduction

The development of food industry over the last century broadened the range of available food products and increased the awareness of society regarding the importance of a healthy diet. As a direct consequence of this, norms and regulation regarding the composition of different products were formulated and are enforced. Still, different food products have a very short shelf-life (*i.e.* fruits and vegetable) and accordingly, their analysis should be performed in a time and price effective way, while maintaining a high standard for the quality and reliability of the analysis.

The current gold standard analytical technique for most of the food products is high performance liquid chromatography (HPLC) combined with different detection schemes such as UV-Vis spectroscopy, fluorescence spectroscopy or mass spectrometry. There are, however, analytes where HPLC-based measurements encounter difficulties and research is still needed in order to overcome these. For those molecules, analysis based on biological assays are applied as reference analytical method.

The objective of the present thesis was to investigate the applicability of surface enhanced Raman spectroscopy (SERS) for the analysis of food products. In order to evaluate the potential and limitations of SERS toward these applications, the thesis is divided in two parts. First, different SERS-active substrates were tested and characterized in order to decide on the best-suited substrate for the development of the analytical procedure. While doing this, the substrates' homogeneity and not their enhancement properties was prioritized. This is thoughtfully discussed in the first part of the results section of the thesis. Second, two selected applications, with increasing degree of complexity, were developed. In both situations a complete analytical procedure is introduced, starting from a thoughtfully understanding of the molecules fingerprint and ending with the measurements and analysis of food extracts. In the first application the

tested food product was a market-available fortified cereal and in the second application, different garden-grown tomatoes were analyzed.

Einleitung

Neben der stetig wachsenden Lebensmittelindustrie und dem damit verbundenen Anstieg der Vielfalt von Lebensmitteln, erhöhte sich in der jüngeren Geschichte auch das Bewusstsein für eine gesunde Ernährung in der Bevölkerung. Dies führte zur Formulierung von Normen und Vorschriften, die die Zusammensetzung unterschiedlicher Produkte festlegt. Um deren Einhaltung zu überwachen, werden kostengünstige und, unter dem Gesichtspunkt der kurzen Haltbarkeit vieler Lebensmittel, schnelle analytische Methoden benötigt. Dabei muss die Methode dennoch hohen Qualitätsstandards genügen und zuverlässige Resultate liefern.

Der derzeitige Goldstandard zur analytischen Untersuchung von Lebensmitteln ist die Hochleistungsflüssigkeitschromatographie (englisch high performance liquid chromatography, HPLC) in Kombination mit unterschiedlichen Detektionsmethoden, wie der UV-Vis-Spektroskopie, Fluoreszenzspektroskopie oder Massenspektrometrie. Für gewisse Analyte sind die Ergebnisse HPLC-basierter Messungen allerdings nicht aussagekräftig genug und weiterer Forschungsaufwand ist vonnöten, um dort Fortschritte zu erzielen. Daher sind für diese Fälle nach wie vor biologische Assays der Goldstandard.

Die vorliegende Arbeit beschäftigt sich mit der Frage nach der Anwendbarkeit der oberflächenverstärkten Raman-Spektroskopie (englisch surface enhanced Raman spectroscopy, SERS) zur Untersuchung von Lebensmitteln. Um das Potential von SERS diesbezüglich beurteilen zu können, wurde die Arbeit in zwei wesentliche Abschnitte unterteilt. Zuerst wurden unterschiedliche SERS-aktive Substrate getestet und charakterisiert, um das geeignetste Substrat zur Analyse von Lebensmitteln zu finden. Hier lag der Fokus allen voran auf der Homogenität der Substrate und weniger auf deren Verstärkungseigenschaften. Auf dieses Vorgehen wird zu Beginn des Ergebnisteils ausführlich eingegangen. Anschließend wurden zwei konkrete Applikationen, mit steigender Komplexität, entwickelt. Das erste Anwendungsbeispiel bezieht sich auf angereicherte Cornflakes, die auf dem Markt frei erhältlich sind. Tomaten aus Gartenanbau

wurden als zweite Applikation untersucht. Beginnend mit der Bestimmung des molekularen Fingerabdrucks, bis hin zur Messung von Lebensmittelextrakten und der Datenanalyse, werden hierfür vollständige Analyseverfahren vorgestellt.

1. Basics

1.1. Why to analyze food?

Over the last couple of centuries, more and more attention has been directed towards understanding the functioning and necessities of the body in order to establish a healthy, dynamic everyday life-style and to increase the awareness towards well-being self-ensuring.^{1, 2} Among others, the investigation of the role, pathway and interactions different molecules have in the mammalian organism upon ingestion has gained much attention and has led to an increased awareness of the importance of individualized diet for allowing people to reach goals such as healthy life, sports performance or body weight.²⁻⁵ Nevertheless, in order to establish dietary plans, information regarding food's composition (amounts of nutrients, vitamins, antioxidants, etc.), shelf life and safety are required. Providing and checking all this data became more and more challenging as food industry developed and the range of possible food choices increased. Still, the higher the range of products, the more important it became to ensure that enough information regarding each product's composition and specifications are available. Accordingly, routine analysis of food became a must for confirming the advertised quality of each available product. In order to establish and implement norms regarding the admitted and recommended values of the different food constituents, organizations such as the European Food Safety Authority (EFSA)⁶ or U.S. Food and Drug Administration (USFDA)⁷ were formed. At the same time, different technologies have been developed toward routine, reliable and fast food analytics (*i.e.* high performance liquid chromatography – HPLC; micro-biological assays; thin layer chromatography; capillary electrophoresis; spectrophotometry)^{2, 8-11}. The choice regarding the most suitable analysis is done on a product-by-product basis. There are a few important aspects that must be considered when choosing an analytical tool or designing an experiment for food analytics:

- Different products have different shelf lives. While a package of biscuits may have a shelf life as long as one year, berries and other fruits might have a shelf life as short as a few days and fresh milk products might only be stored a few

hours without refrigeration.¹² Ensuring that an analytical method would be available on site to meet the shelf-life requirement is vital.

- Physical properties and exact composition of raw food (*i.e.* fruits, vegetables, meat, etc.) depend on factors such as temperature, pressure, moisture, harvesting time, harvesting procedure and storage conditions.¹⁰

- Raw materials undergo a phase transformation during processing, leading to chemical changes (*i.e.* the lycopene content in fresh tomato fruit, canned tomato paste and dried tomato stored in essential oil are not identical;¹³ moreover, the lycopene content in canned tomato paste provided by different producers might differ substantially). Accordingly, individual tests of different products are required.

- During food culture different pesticides are added to the plants to fight plant-insects and plant-diseases. Moreover, different coloring agents might also be added in order to enhance the fruit colors and to produce more appealing food products. Similarly, growth agents and antibiotics are added to the animal food. Trace amounts of these additives can still be detected in the final product and may cause diseases or discomfort.^{14, 15} Accordingly, strict legislations have been formulated in order to define the safety of consuming the affected products and routine analyses are needed to enforce these norms.^{6, 7}

- During processing, different conservation agents or antioxidants are added to food in order to increase their shelf-lifetime.^{2, 8, 14} Still, there are strict legislations regarding the usage of food additives as well as preservatives and routine analyses are required for ensuring that a safe amount of food preservatives is added.^{6, 7}

- There is a high demand for hygiene when working with raw food (*i.e.* meat and milk products) and overlooking this may lead to the spread of different diseases.^{16, 17} In order to prevent such an event, strict norms are imposed in the food production, processing and commercializing stages. Routine analyses of the final product are also required.

- Food products are different from pure substances in the sense of being complex combinations of pure substances with varying compositions.¹⁰ This

requires additional attention and work regarding the analysis of the target product or target analyte inside the product.

All the aspects mentioned above lead to a strong requirement of individually considering each substance present in a food matrix when opting for an analytical tool. That is because the food matrix is a complex system, with interconnected, interdependent constituents and analyzing one of these requires a bigger or lower consideration of its chemical and physical environment. Additionally, care should be taken to the particular features of the studied analyte (*i.e.* ascorbic acid, riboflavin, vitamin A, β -car, vitamin B6, vitamin B12, vitamin D, vitamin K, folic acid, and tocopherols are destroyed when milk-based products containing them are exposed to light for a longer period of time)¹⁸. Last, time, final price and reliability of the analysis is thoughtfully considered when choosing the technology applied for food analytics.

In this thesis, the analytes of interest were two of the eight B vitamins, namely riboflavin (vitamin B2) and cyanocobalamin (vitamin B12), two of the different 600 available carotenoids, namely β -carotene (β -car, also known as pro-vitamin A) and lycopene (lyc) and vitamin A. As a starting point, a short characterization of these molecules, their bioavailability, their pathways upon ingestion and roles in mammalian's well-being is provided.

1.1.1. Vitamins B2 and B12 and their dietary importance

The B vitamin complex consists of eight distinct chemicals: thiamine (B1), riboflavin (B2), niacin (B3), pantothenic acid (B5), pyridoxine, pyridoxal, pyridoxamine (all different forms of B6), biotin (B7), folic acid (B9) and cyanocobalamin (B12), which can be found in the same food products (*i.e.* milk, cheese, eggs, dark-green vegetables, fruits, liver, kidneys, legumes, mushrooms, almonds)¹⁹. The one important exception is B12, which is only available from animal derived dietary sources (*i.e.* meat (especially liver), fish and shellfish, poultry and milk products)²⁰, leading to an increased risk of strict vegetarians (vegans) to develop health problems. Yet another group that encounter problems assimilating both B2 and B12 and are exposed to an increased risk of developing deficiencies are elderly, pregnant women and teenagers.²⁰⁻²² Among the different

possible consequence these deficiencies range from anemia (for both B2 and B12), eye fatigue, extreme unusual sensitivity to light (B2), a swollen dark-colored tongue (B2), digestive problems (B2) to cardiovascular diseases (B12), depression (B12), paranoia and dementia (B12).^{20, 21, 23-27} It is, accordingly important to ensure a healthy uptake of this two vitamins (recommended daily amount of B12 is estimated to be 1.5-3 μg and for B2 it is 1-1.4 mg).^{21, 23, 28} The main path for this is through vitamin supplements or by consuming fortified foods (*i.e.* fortified cereals for breakfast)²⁹. In the case of fortified foods information regarding composition of food is required. In order to reliably acquire this information two different analyses are routinely performed: HPLC coupled with fluorescence detection for the identification and quantification of B2 and micro-biological assays using *Lactobacillus delbrueckii* as the test microorganism for the detection and quantification of B12.³⁰

1.1.2. Dietary benefits of β -car and lyc

Carotenoids are plant-synthesized chemicals with a high bioavailability (there are more than 600 different carotenoids responsible for the different plant functions)^{31, 32} and important roles for the mammalian organisms. Their function upon intake range from regulation of cell transcription, regulation of gap junctional intracellular communication, reduction of oxidative stress and antioxidant activity to pro-vitamin A activity.³³⁻³⁵ It was found that around 50 carotenoids are present in the human diet and only 5-6 of them have been identified in the human plasma (α - and β -car, β -cryptoxanthin, lyc, lutein and zeaxanthin).^{33, 34, 36} Moreover, from these six, all-*trans*- β -car is the only one that can be cleaved into two all-*trans*-retinal molecules (vitamin A).³⁴ This is mostly (but not exclusively) occurring at the intestinal level by the action of the enzyme β -car-monooxygenase-1 (BCMO1) and, according to the available literature, it appears to have a feedback regulation property, making β -car an effective help against vitamin A deficiency.^{31, 34, 37-39} As compared to β -car, lyc has no pro-vitamin A activity, but it has the highest efficiency in neutralizing reactive oxygen species (ROS) and its activity leads to a reduction of the cell-division at the G0-G1 cell cycle phase by regulating the gap junctional intracellular

communication.^{33, 35, 40} Due to this, lyc is considered to play an important role in decreasing the risk of cancer development.⁴⁰ The important, yet different functions carotenoids have upon ingestion lead to the necessity of a good identification and quantification of them in food products in order to decide on the best diet for different individuals. Still, during the different stages of plant growth more than just one carotenoid is present. Moreover, carotenoids iriversally transform into each other at different stages of the plant lifetime. A schematic of this process is depicted in **Figure 1** (for just the 6 carotenoids also detectable in human plasma). As observed from this figure, the chemical structures of the different carotenoids resemble strongly, making the identification/quantification rather challenging. The gold standard for carotenoid analysis currently is HPLC coupled with mass spectrometry (MS).⁴¹

1.2. State of the art in food analytics

HPLC coupled with different detection methods (*i.e.* UV-Vis spectroscopy, diode array, MS, etc.) has developed into a powerful analytical tool capable of analyzing complex mixtures of substances in real time.⁴² Moreover, according to the available legislation (enforced by organizations such as EFSA⁶ and USFDA⁷) HPLC is currently the gold standard analytical method for the analysis of most food relevant molecules.^{36, 43} There are, however, analytes where chromatography-based measurements encounter difficulties due to co-elution^{44, 45} and research is still needed in order to overcome this. For those, biological assays analysis still is the reference analytical method.⁴⁵

1.2.1. HPLC

HPLC is based on a relatively simple concept first reported more than a century ago:⁴⁶ molecules' simultaneous interaction with liquid and solid substances. Basically, a molecule dissolved in a solvent and passing through a column of solid particles will physically and chemically interact, to different degrees, with both the solid particles (referred to as the stationary phase) and the initial solvent (referred to as the mobile phase) . Depending on the solubility of the

molecule, its size and the size and nature of the particles in the column, the molecule might fast exit the column, be delayed or remain absorbed on the particles inside the column.^{36, 41, 47} Further on, if a solvent having a different polarity is later passing the same column, the molecule will, most probably exit the column together with this solvent. Based on this concept, different mixtures of analytes can be separated by adjusting the solvent sequence and carefully choosing the length of the column and the type of solid particles inside it. Further on, upon development of this principle and by using a sequence of pressurized solvents for the separation, HPLC (initially named high pressure liquid chromatography) was developed. Still, as described above, HPLC is a separation method and not a quantification one.^{36, 47} In order to analyze and quantify the emerging substances a detection method is used *in line* with HPLC. Depending on the nature of the analytes of interest different detection methods are used: UV-Vis spectroscopy, diode array, mass spectrometry, etc.^{36, 41, 42, 44} The resulting analytical system is generally able to perform reliable, reproducible, time effective analysis of complex mixtures of analytes. The drawback of this method is often the price due to (i) the initial cost of the HPLC system, (ii) the price of the detection system (depending on the particular requirements of the analytes of interest) and (iii) the price of the reagents used for calibration.^{44, 47} Further on, the technique might encounter problems with co-elution when the analytes of interest are very similar and not enough consideration is given to achieve a good separation or the needed columns are not available.^{44, 47} Moreover, additional costs are required for the systems' maintenance and most of the analytical procedures used for HPLC are in-house developed and differ from one lab to another, making the lab-to-lab comparison challenging. One situation in which HPLC is currently used as gold standard analytical tool is the analysis of different carotenoids. More specifically, lyc is known to have a very short shelf life (storage requirements: dry, dark, oxygen free space, -70°C and for the case of stock solutions the exact shelf life depends on the exact lab conditions and handling procedure) and a high price (~180 euro/mg for the case of lyc according to Sigma Aldrich). Still, prior to each HPLC analysis of the lyc content of a food sample, a system calibration measuring different concentrations of a standard lyc solution is required.

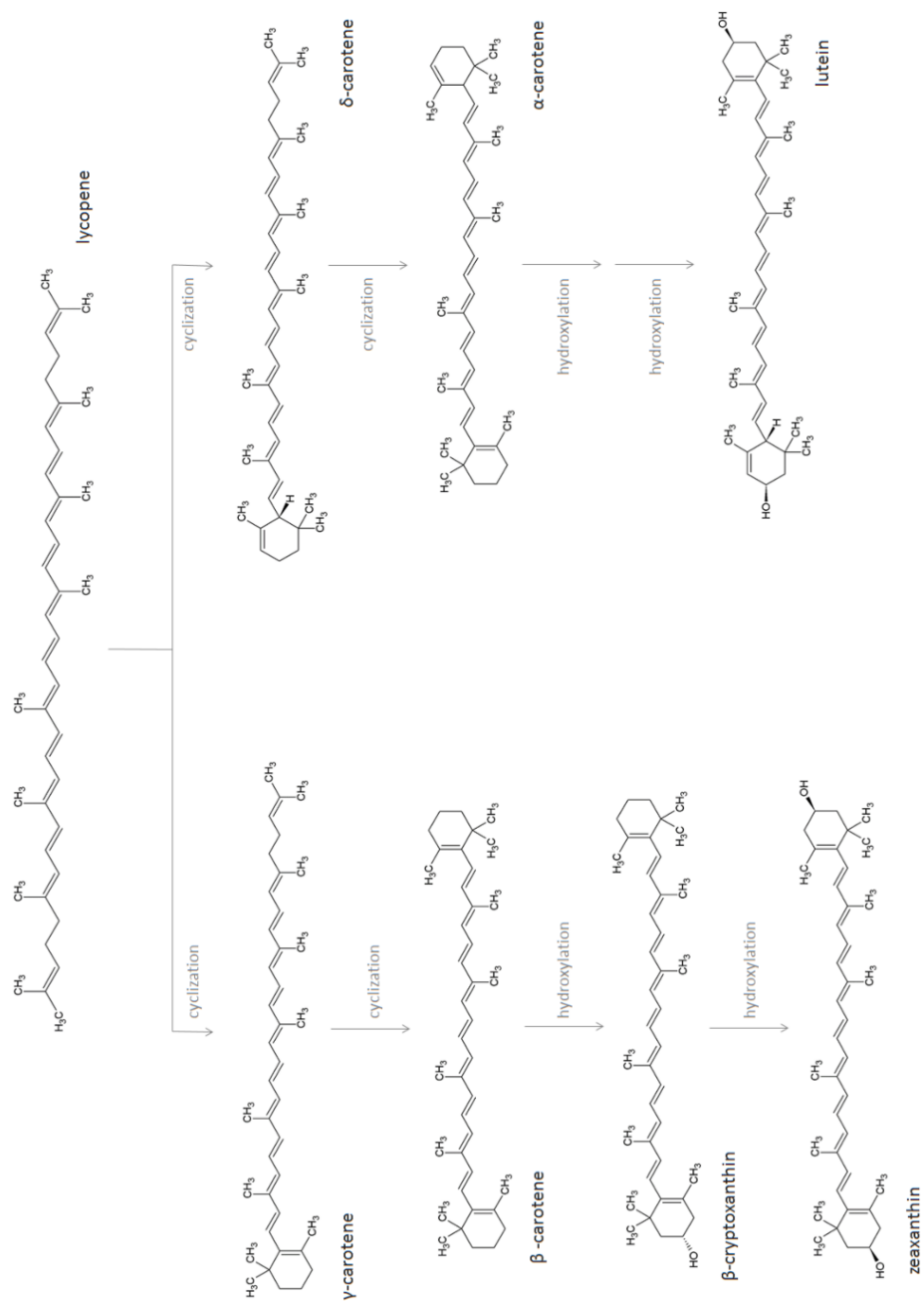


Figure 1 A simplified scheme depicting the conversion of lyc to β -car. A larger carotenoid conversion schematic is depicted and described by G. A. Armstrong⁴⁸ *et al.* and J. Hirschberg *et al.*³²

1.2.2. Microbiological assay

Microbiological assays have been developed for the sensitive and specific detection of amino acids, vitamins and antibiotics. Basically, the concentration of the test analyte is determined based on the growth of a test microorganism.^{45, 49-51} In the case of vitamin B12 *Lactobacillus delbrueckii* is used as the test microorganism because it was found that the vitamin is required for the growth of this microorganism. In order to get quantifiable results a food extraction is performed and the obtained solution is used for preparing a growth media for the *Lactobacillus delbrueckii*. The growth rate of the microorganism in the this media is afterwards compared with the results of the microorganism's growth in precisely controlled experiments (containing known amounts of B12).⁵⁰ The main drawback of this procedure is the total time needed for obtaining the results (~26 hours at least), making the technique not feasible for fast analysis.⁵¹ The reliability of the measurement, however, is high: microbiological assay analysis of vitamin B12 being the gold standard method for quantification of B12 in food products.^{30, 45}

1.3 SERS – an emerging technique for the field of food analytics

Discovered more than 40 years ago, SERS provides fingerprint identification of trace amounts of analytes in real-time having the potential to develop toward routine analysis of various compounds (*i.e.* water pollutants, food components, antibiotics, etc.).⁵²⁻⁵⁸ In a simplified approach, this is achieved because of the interaction of light with metallic nanoparticles or nanostructures ($\lambda \gg d$). Upon this interaction, surface plasmon resonances (SPR) are excited and a strong electromagnetic field is generated at the metal-dielectric interface. The strength and exact frequency at which the SPR are generated depends on the morphology and the material of the substrate, the surrounding dielectric medium (*i.e.* air, water, oil, etc) and the incident laser wavelength.^{56, 58} As a direct consequence, the localized surface plasmon polariton (LSPP – the resonant excitation associated with a local field enhancement) of a SERS substrate can be tuned by adjusting the composition, shape, size, and the inter-particle spacing of the nanoparticles. Furthermore, in the case of planar metal surfaces under the

appropriate experimental conditions (Kretschmann or Otto configuration) propagating surface plasmon polaritons (PSPP) can also be induced at boundaries between the nanostructured metal and the dielectric. Because of the evanescent character of the localized electromagnetic field, the Raman signal of molecules located in the close vicinity (roughly 10 nm) of the nanostructure can be enhanced by several orders of magnitude.^{56, 57, 59-61} This accounts for the electromagnetic enhancement mechanism contribution to the SERS effect. The second, much weaker, mechanism contributing to the SERS effect is the chemical enhancement. The last includes enhancement due to either the interaction between the nanoparticle and the molecule in the ground state, the resonance enhancement of a surface complex or due to the photon-induced charge-transfer (PICT).^{56, 58}

Apart from this, it is also important to mention here that the fingerprint identification of molecules by means of SERS is possible due to the interaction of the molecules with the electromagnetic radiation. SERS and Raman spectroscopy detect the electromagnetic radiation in-elastically scattered by the molecules. Briefly, upon the interaction of light (ω_0) with a molecule, different processes can occur. Among them there is the scattering of photons either elastically (referred to as Rayleigh scattering) or in-elastically (referred to as Stokes scattering if $\omega_s = \omega_0 - \omega_{\text{vib}}$ and anti-Stokes scattering if $\omega_s = \omega_0 + \omega_{\text{vib}}$)^{62, 63}. Due to the fact that the energy of the incident photon ($\hbar\omega_0$) is generally not equal with the energy required for an electronic transition, this energy is not absorbed by the molecular system, but only virtually absorbed to a virtual state and then re-emitted.^{61, 62} If the energy of the emitted photon is lower than the one of the absorbed photon Stokes Raman scattering occurs. If, however, the energy of the emitted photon is higher than the one of the absorbed photon anti-Stokes Raman scattering occurs. Either way, the measured spectrum contains information about the molecular vibrations. Finally, if the energy of the incident photon is equal to the energy required for an electronic transition resonance Raman occur.^{61, 63}

SERS has been mainly used as a laboratory tool so far, but more and more studies are directed toward developing routine analysis using SERS.^{15, 56} Still, in order to develop applications a few aspects must be considered, starting with a fundamental understanding of the requirements for performing SERS measurements (*i.e.* nanostructured substrates, laser wavelengths, a spectrometer,

etc.), the decision regarding the best-suited SERS-active substrate and ending with the development of the much needed chemometric-based tools for fast analysis of the experimentally acquired data.

1.3.1. Requirements for performing SERS measurements

As mentioned, there are two main, interconnected requirements for performing SERS measurements: the decision regarding the best-suited SERS-active substrate and the availability of a Raman measurement system for performing the measurements. As largely discussed in the literature,^{56-59, 61} a SERS-active substrate is a metallic ‘nanostructure’ that can have different sizes (within the nanometer range), different shapes (*i.e.* spheres, rods, nano-holes, rectangular nanowires or different gratings) and different degrees of roughness. In addition, it can be presented as a colloidal solution or as a solid substrate and it can be functionalized with well-defined capture molecules. Depending on the preparation procedure, the SERS substrates can be separated into bottom-up substrates, self-organizing substrates and top-down substrates.^{56-58, 60, 64} Among the reported metal nanostructures fabricated by bottom-up procedures there are metal colloids^{65, 66}, core-shell nanoparticles and structures^{67, 68} as well as seed mediated growth structures^{69, 70}. Metallic colloid solutions have been intensively studied and different sizes, geometries as well as functionalization of nanoparticles have been achieved. However, the main drawbacks of these procedures are often the broad size and shape distribution and the solvent used (water). Due to the solvent being water, these colloidal solutions cannot be directly applied for the measurement of different fat soluble food analytes such as vitamin A or E. Moreover, due to the size heterogeneity the LSPP band of the obtained colloidal solutions is rather wide. To account for this, additional substrate preparation steps might follow, resulting, among others, in an increase of the size/shape homogeneity, in different functionalization, core-shell structures, and change of the solvent or immobilization of the nanoparticles on a substrate. Still, this further increases the complexity of the preparation protocol.

Further on, among the mentioned substrate preparation techniques, the self-organizing substrates on the other hand include self-assembled nanoparticles^{71, 72},

clusters and arrays as well as template based self-assembled nanoparticles⁷³⁻⁷⁵ while the top-down substrates include template preparation by means of electron beam lithography (EBL)^{76, 77}, lift-off processes^{78, 79}, ion etching and ion beam etching processes as part of lithographic methods^{80, 81} as well as nanoimprint lithography^{82, 83}. Among these, the top-down techniques are less cost effective and the preparation protocol is more complex, but they often result in highly reproducible, highly structured substrates. Moreover, in many cases, the as prepared substrate can be stored over time and the final layer of the coinage metal (i.e. Ag, Au, Cu or Pt) can be deposited on the substrate short before usage.

Accordingly, a high variety of substrates is available and the resulting substrates also have different properties. As expected, in this situation the choice of the best-suited SERS substrate is not trivial. As mentioned before though, besides the complexity and reproducibility of the preparation procedure, the time and price requirements and large-scale homogeneity of the substrates' nanostructure, other factors should also be considered. Among these, there is the system requirements for the SERS measurements, including the availability of the laser wavelength needed for the LSP excitation and, most importantly, a thoughtfully consideration of the desired application. The last one is of particular importance as depending on the application, different microfluidic systems, a one-time-easy-to-use substrate or a recyclable substrate might be best-suited. Accordingly, when deciding on the SERS-active substrate that is to be used in an application, one should be looking for the best-fitting substrate for the specific application and not for a universally best SERS-active substrate.

1.3.2. The best-suited SERS-active substrate for food analytics

First tests regarding the application of SERS for food analysis are already available in the literature^{15, 84-87}. For example, V. Peksa *et al.*¹⁴ developed a SERS-based procedure for the fast estimation of azorubine dye in sweet drinks. Also, M. Jahn *et al.*⁸⁴ developed a SERS lipophilic sensor for the detection of sudan III dye in spiked paprika extracts. However, these different studies only introduce first tests toward establishing SERS for food analytics and much work is still required to reach a final conclusion regarding this. That is because, as already mentioned, the

food matrix is a complex system, with interconnected, interdependent constituents and analyzing one of these requires a bigger or lower consideration of its chemical and physical environment. Moreover, fast, cost-efficient and reliable analyses are required in order to provide customers with a fresh, safe product.

Due to the high variety of available substrates and due to the different properties each substrate has, a good theoretical characterization of the substrate considered for a particular characterization is required in order to define the best fitting measurement conditions.⁵⁷ Upon this, the applied laser wavelength can be chosen to account for the resonant excitation of the LSPP and (if possible) PSPP. Further on, a given SERS-active substrate may provide for a reliable, reproducible detection of the target analyte on the substrate's surface.^{61, 64, 88} Depending on the exact features, the substrate might be better suited for a specific application (*i.e.* a substrate with a relatively uniform enhancement will generally be suited for applications that require quantification and a high reproducibility of the measurement while a substrate that does not account for a relatively uniform enhancement would often present spots with higher enhancements, being better suited for applications connected to single molecule detection).^{58, 61}

For the development of SERS toward fast, reliable analysis (*i.e.* routine analysis of food or water pollution) the batch-to-batch reproducibility of the preparation protocol and the complexity, time and price requirements of this procedure^{88, 89} are also important. Additionally, in an ideal situation, the prepared SERS substrate is expected to have a long shelf life, as this would allow for the fabrication of the substrate at a time prior to the actual application.^{58, 88} Yet another factor considered when choosing the "optimal" SERS substrate is the metal used for substrate preparation. As most of the applications are designed towards the visible/near-infrared range (400-1000 nm) the most commonly used enhancing metals are silver (Ag) and gold (Au).^{61, 89} However, when choosing in between those two, the long-term stability of the substrate, the substrates price, enhancement, the targeted wavelength for the application and the target analytes chemistry are considered. More exactly, it is well known that Ag oxidizes easily, making the substrates storage rather challenging as compared with the storage of Au-based substrates. Furthermore, gold is more chemically inert, which is important in applications such as cell measurement.⁹⁰ However, by using Ag the

final price of the SERS-active substrate is lower. Moreover, the strength of the LSPR of Ag is higher than the one of Au. To understand this, the dielectric function of the two materials has to be considered. More exactly, the real part of the dielectric function of the two is comparable due to the similar electronic densities of Au and Ag⁹¹, but the imaginary part of this function has a higher magnitude for the case of Au, resulting in a higher absorption at wavelengths lower than 600 nm.⁶¹ Therefore, at wavelengths lower than 600 nm the LSPR of small gold nanoparticles are damped. For the case of bigger nanoparticles, however, the resonances shift towards wavelengths higher than 600 nm. Still, at high nanoparticle sizes radiation damping occurs.⁶¹ Accordingly, the typical wavelengths where substrates have been established to support SERS are 400-1000 nm for Ag and 600-1300 nm for Au.⁸⁹ Finally, as mentioned, the analyte chemistry should also be closely considered as the presence of oxygen and nitrogen groups facilitates the molecules absorbance on Ag substrates while oxygen, nitrogen and sulfur groups are also easily absorbed on Au substrates.⁹² The latest is important to achieve, as the establishing of a chemical bounding of the target analyte to the substrate is crucial for measurements performed under dry conditions if a washing step is taken after incubation of the substrate in the analyte solution.^{52-54, 59, 60} Moreover, by choosing the “optimal” substrate/analyte combination the resonant conditions can be also achieved for the analyte measurement, leading to a resonant SERS (often denoted SERRS).⁶¹

In conclusion, to develop SERS toward a routine food analytical tool different factors have to be considered. First, the used SERS-active substrate should provide a uniform, good enhancement, with no more than 20% deviation over the surface of the substrate.^{58, 61} As an extension to this, the preparation reproducibility of the substrate should be also high (less than 20% batch-deviation).⁵⁸ Second, the SERS-active substrate should be easy to store (should have a long shelf life), easy to prepare on the spot or both.⁵⁷ Third, the final preparation protocol should, ideally, be cost-effective.⁵⁷ Further on, as mentioned before, the SERS-active substrate should be used in combination with a commercially available laser wavelength. The Raman system used for the measurements should, ideally, allow for on-field measurements and, consequently, the measurement procedure should be rather simple.

All these different aspects were closely assessed during the first part of the work introduced within this thesis. Moreover, the assessment of the best-suited substrate for food application was done based on the list introduced in this paragraph.

1.3.3. Chemometric-based tools for fast food analysis

Upon designing the experimental procedure and acquiring the experimental data, a further, important step consists in its analysis and interpretation. The data analysis should ideally be automated, fast and easy to perform. While much work is required in order to develop and implement such a procedure, the application of such a final analytical tool leads to relatively low expertise requirements for the operator.

To achieve this, however, chemometric methods such as multivariate calibration (*i.e.* partial-least squares regression – PLSR⁹³⁻⁹⁵, or principal component regression – PCA⁹³⁻⁹⁵), classification, pattern recognition and clustering of the data (*i.e.* discriminant analysis on principal components^{96, 97} or partial least squares scores^{98, 99}) should be introduced in the routine data analysis. To establish such a procedure, a relatively high number of input spectra are required for the training of the analytical, chemometrics-based model. Still, the training data set would, ideally, be acquired at a day prior to the actual food testing and the chemometric based (*i.e.* regression) result could be afterward applied at any required time. In order to ensure for this, though, an external standard has to be implemented in the measurement and analytical procedure to account for day-to-day data comparison by performing a wavenumber calibration. Additionally, to account for all the different measurement system errors, an internal standard should also, ideally, be implemented. Upon these, the SERS measurement and data analysis for one food sample should not require much time. More exactly, once the chemometrics-based data analysis is developed and the time required for the analysis of a food sample would only consist of a sum of the time needed for performing the food extraction, the SERS measurement (ideally, not more than 30-60 min) and the data analysis itself (ideally, not more than 5-10 min).

2. Materials and methods

2.1. Chemicals and reagents

All reagents were of analytical or HPLC reagent grade. Retinol (vitamin A, $\geq 95\%$ pure), β -car (pro-vitamin A, $\geq 95\%$ pure), lyc ($\geq 90\%$ pure), Nile blue (NB), butter yellow (BY, $\geq 98\%$ pure), riboflavin (vitamin B2, $\geq 98\%$ pure), cyanocobalamin (vitamin B12, $\geq 98\%$ pure), 2,6-di-tert.-butyl-4-methylphenol (BHT, $\geq 99\%$ pure), α -amylase (from *Bacillus subtilis* po, 50 units/mg activity), starch (from potato, p.a., ISO, Ph. Eur.), hydrochloric acid ($\geq 98\%$ pure), Taka-Diastase (from *Aspergillus oryzae*), silver acetate (99%) were purchased from Sigma Aldrich (Steinheim, Germany). Tetrahydrofuran (THF, $\geq 99,9\%$ pure) and sodium acetate trihydrate (p.a., ACS, Reag. Ph. Eur.) were purchased from Merck KGaA (Darmstadt, Germany). Methanol ($\geq 99,5\%$ pure), *n*-hexane ($\geq 99\%$ pure), D(+)-sucrose ($\geq 99,5\%$ pure), D(+)-water-free glucose (p.a., ACS), D(-)-fructose ($\geq 99,5\%$ pure), acetic acid ($100\geq\%$ pure), acetone ($\geq 99,5\%$ pure), ethanol ($\geq 99,5\%$ pure), hydroquinone and hydrogen peroxide (30%) and microscope glass were purchased from Carl Roth (Karlsruhe, Germany). Ascorbic acid (vitamin C) and silver nitrate (AgNO_3) were purchased from EMD Millipore Corporation. HD DVD (Hitachi video) disk was purchased from Amazon.co.uk. Distilled water was produced in-house.

Fortified cereals used for the study were purchased from local stores from the area of Jena, Germany. Cherry tomatoes at different ripening stages were provided by local producers from the area of Jena, Germany. First, a series of four tomatoes (series A) exhibiting different degrees of ripeness (yellow to red) were taken from the same tomato plant. The tomatoes were immediately frozen and stored at -20°C till analysis. A second series of four tomatoes (all of them exhibiting the same degree of ripeness – all yellow) were gathered from one plant (series B). One tomato from this batch was frozen immediately. The remaining tomatoes were illuminated with an 11 W lamp for various periods of time leading to increasing degrees of ripeness. After illumination the tomatoes were frozen and stored at -20°C .

2.2. SERS active substrates

2.2.1. Enzymatically generated silver nanoparticles (EGNPs)

In order to prepare enzymatically generated silver nanoparticles (EGNPs) the protocol described by S. Yüksel *et al.*¹⁰⁰ was used. Briefly, glass slides were stepwise cleaned in an ultrasonic bath using acetone, ethanol, and distilled water. Then, a 20 μM single-stranded biotinylated DNA (dissolved in 5 \times phosphate buffered saline (PBS)) was spotted on the glass surface. The glass slides were then exposed for 10 min to UV light (254 nm) to ensure binding of the DNA molecules to the glass surface. Next, the glass slides were washed for 10 min with 0.1 \times saline-sodium citrate/0.5 sodium dodecyl sulfate. Upon this, the substrates were incubated for 1 h at room temperature in 1 \times PBS/0.05% Tween (PBST). As a consequence of the interaction of biotin and streptavidin during this time, a streptavidin horseradish peroxidase (HRP) conjugate complex was bound to the surface through the linker molecule. Upon this step, the substrates were washed six times with PBST for 2 min. This lead to the removal of all unbound enzyme. Finally, the substrates were incubated for 5 min in a solution containing H_2O_2 and silver acetate in distilled water solution and hydroquinone (HQ) in citrate buffer. After 5 min the reaction was stopped by rinsing the substrates with distilled water and they were dried with compressed air.

Scanning electron microscopy (SEM) images of the prepared SERS-active substrates were taken with a Hitachi S-4800 instrument.

2.2.2. “Nanosponge-like” substrates (NSs)

“Nanosponge-like” substrates (NSs) were prepared according to the protocol described by D. Wang *et al.*^{101, 102}. Briefly, Au/Ag bi-layers (10 nm Au and 20 nm Ag) were deposited on SiO_2/Si substrates (1 \times 1 cm^2) using electron beam evaporation. Then, thermal annealing induced dewetting (900 $^\circ\text{C}$ and Ar atmosphere) was performed for 15 min in order to form Au-Ag alloy nanoparticles. Following this, the resulting samples were submerged for 5 min in a 65 wt% HNO_3 aqueous solution at room temperature for dealloying. As a result,

the less noble element (Ag) was removed resulting in the formation of Au nanosponges (Au NSs).

In a next step, the Au NSs were immersed for 5 min in 10 mM ascorbic acid at room temperature. During this time, the reducing agent was adsorbed in the sample's "nanosponge-like" structure by capillary effects. Upon this, the samples were rinsed with deionized water and immersed for 5 min in 5 mM AgNO₃ solution, at room temperature. This induced the reduction of Ag⁺ ions and the formation of an Ag coating layer. Upon this, the substrates were washed with deionized water and the above process was repeated another 5 times resulting in the formation of Ag/Au nanosponges (Ag/Au NSs).

SEM images of the prepared SERS-active substrates were taken with a Hitachi S-4800 instrument.

2.2.3. HD-DVD-based substrates

In order to prepare HD-DVD-based substrates (HD-DVDs) the protocol described by A.I. Radu *et al.*¹⁰³ was used. Briefly, double-sided HD-DVD disks have encoding pits molded into the two 0.6 mm thick polycarbonate (PC) layers separated by two reflective, 0.1 mm, mirror-like metal films in between which an additional thin, polymer-based protective layer is situated. The encoding pits are nanostructures having 250 nm width, 200–1000 nm length, 35–80 nm depth and are spatially distributed in concentric rings with a period of 400 nm. This PC layer was used as template for preparing SERS active substrates. To do so, the HD-DVD disks were separated using a sharp knife and the reflective metal film was removed with scotch tape. Following this, the PC template was cleaned and an Au layer was sputter-coated. The resulting substrates were cleaned by 5 min oxygen plasma treatment to remove organic contaminations. Finally, the disks were divided in 5×5 mm small substrates.

SEM images of the prepared SERS-active substrates were taken with a Gemini 1530 LEO field emission microscope.

2.2.4. EBL-based substrates

In order to prepare EBL based substrates (EBL substrates) the protocol described by U. Huebner *et. al.*^{76, 104} was used. Briefly, for the development of the substrates e-beam lithography, vacuum evaporation and ion-beam etching were used. Two slightly different structures were prepared. For this, slight differences in the applied protocols were used. The differences are marked in **Table 3** and the common preparation protocol is described as follows: a 4" fused silica wafer was cleaned using peroxymonosulfuric acid solution and then a thin undercoating (HMDS) and a defined thickness (see **Table 3**) of a negative tone electron beam resist (see **Table 3**) were spun on the wafer. The resist was baked for 3 min at a controlled temperature (see **Table 3**) on a hotplate. A 10 nm gold layer was evaporated on top of the resist. The electron beam exposure, which was performed by using the unique character projection based electron beam technique¹⁰⁴ of the shaped beam writer SB350OS (from Vistec Electron Beam GmbH), resulted in the formation of fixed number of chips/wafer (chip size: 5x10 mm² - see **Table 3**). Each of the obtained chips contains 4 gratings with a size of 1 x 1 mm² for the SERS investigations. The exposure and the removing of the gold layer were performed afterwards. This was followed by the development of the resist as described in **Table 3**. Next, the etching into the fused silica surface was done with a CHF₃-SF₆-ICP etching process (Inductively Coupled Plasma - ICP) by using ICP power of 300 W. The etch depth of the 2d gratings with a fixed period (see **Table 3**) is around 100 nm. Last, the residual resist was removed using oxygen plasma and the wafer was separated into single chips. Finally, Ag films were deposited freshly (at the beginning of every measurement day) by means of thermal evaporation at an oil-free background pressure in the lower 10⁻⁷ mbar range. For this, high-purity silver granules were used as raw material. The thickness of the silver layer was 40 nm.

SEM images of the prepared SERS-active substrates were taken with a JEOL JSM-6700F system.

Table 3 Parameters used for the preparation of the EBL substrates for the measurements of the B vitamins and of the carotenoids.

Parameter	Substrates for the measurements of the B vitamins	Substrates for the measurements of the carotenoids
electron beam resist	‘maN2401’ (micro resist technology GmbH)	‘AR6200.09’ (ALLRESIST GmbH)
electron beam resist thickness	100 nm	260 nm
resist baking temperature	90°C	150°C
chips/wafer	140	48
development of the resist	in AZ MIF 726 developer for 30 s the H ₂ O rinsing for 60 s	in a AR 600-546 developer for 60 s the IPA rinsing for 30 s
grating period	250 nm	436 nm

2.3. Sample preparation

For the characterization of the EGNPs, stock solutions of 10 μM B2 in distilled water were prepared and used for the SERS measurements short upon preparation.

For the characterization of the NSs, stock solutions of 100 μM BY in *n*-hexane and 100 μM B2 in distilled water were prepared and used for the SERS measurements short upon preparation.

For the characterization of the HD-DVDs stock solutions of 1 mM concentration of retinol and β -car were prepared by solving the appropriate powder quantities in *n*-hexane. The solutions were used for the SERS measurements short upon preparation.

For the characterization of the EBL-based substrates stock solutions of 100 μM lyc and 1 μM B2 were prepared by solving the appropriate powder quantities in *n*-hexane and distilled water. The solutions were used for the SERS measurements short upon preparation.

For the development of SERS-based food applications different solutions were prepared and tested. They are described in the paragraphs above.

For the measurement of the B vitamins, stock solutions and dilutions were prepared by solving the appropriate amount of powder in a hydrochloric acid solution of pH 6. These solutions were used for the SERS measurements short

upon preparation, by using a new SERS substrate for each concentration. In between the measurements the solutions were stored at -4°C .

For the estimation of the limit of detection (LoD) of the B vitamins at pH 6, solutions having the following concentrations were prepared and measured: 10 μM , 1 μM , 100 nM, 10 nM and 1 nM. They were kept at -4°C until measurement and a different substrate was used for each measured concentration. The measurements were performed short after the solutions were prepared.

For the measurement of the B vitamin simulated food matrix (BSFM) six components were mixed: glucose (G), fructose (F), sucrose (S), starch, B2 and B12. The ration in which these were mixed was chosen based on the composition of the cereal further investigated. Still, at this point of the experiments, the lipid/protein and salt content of the cereal mix was neglected. **Table 1** presents the cereal mix composition as provided by the producer. The measured BSFM contains 1:9 dilutions of the ones in **Table 1**. For these, an aqueous hydrochloric acid solution of pH 6 was used to prepare stock solutions of G (55.6 mM), F (50.4 mM), S (41 mM) and starch (137.86 mg in 10 ml solvent). For starch, an exact concentration is not provided due to the fact that starch is only slightly water-soluble. As a consequence, the starch suspension was dispersed in an ultrasonic bath for 20 min and centrifuged at 5000 rpm for 5 min and the resulting supernatant was used for the preparation of the BSFM. The final concentrations of the six components in the BSFM are: 100 nM B2, 100 nM B12, 3.31 mM G, 3.31 mM F and 3.31 mM S.

For the estimation of the LoD of the B vitamins solutions at pH 6, in the presence of the BSFM, the following concentrations of the vitamins were tested: 1 μM , 600 nM, 300 nM, 100 nM, 90 nM, 80 nM, 70 nM, 60 nM, 50 nM, 40 nM, 30 nM, 20 nM and 10 nM. For the measurement of each of these, a different substrate was used and the as-prepared solutions were stored at 4°C until measurement (same day).

For the measurement of the carotenoids β -car and lyc were dissolved in a mixed solvent of methanol and THF stabilized with 0.1% BHT (1:1, v/v) to prepare the solutions that were measured. All SERS measurements were performed short upon the solutions were prepared. However, the solutions were

stored at -20°C for the needed time. For each mixture a different substrate was used.

For the estimation of the LoD of the carotenoids, the following concentration range was tested for each of the two carotenoids: 106, 90, 74, 58, 42, 26, 10, 9, 7.4, 5.8, 4.2, 2.6 and $1\ \mu\text{M}$.

For the measurement of the β -car/lyc mixtures stock solutions of $100\ \mu\text{M}$ of each analyte were prepared and mixtures of the two in different percentages were obtained and measured. The exact percentages are presented in **Table 2**.

Table 1 Overview of the composition of cereals as provided by the producers.

Analyte	Concentration		
	quantity/100g cereal	M/l	quantity/ml*
lipids	5 g		5 mg
carbohydrates	82 g		82 mg
- out of which sugars	35 g		35 mg
- out of which starch	47 g		47 mg
fibers	2.5 g		2.5 mg
proteins	6 g		6 mg
salt	0.88 g		0.88 mg
iron	8 mg		8 μg
B1**	0.97 mg	2.70 μM	0.91 μg
B2**	1.2 mg	3.19 μM	1.2 μg
B3**	13 mg	0.108 mM	13.3 μg
B6**	1.2 mg	4.91 μM	1.2 μg
B9**	334 μg	0.376 μM	0.334 μg
B12**	2.1 μg	1.55 nM	0.0021 μg

* value recalculated based on the content in the extract (10 g cereal/100 ml solution)

** vitamins

Table 2 Percentages of β -car and lyc in the measured mixture solution and afferent concentration of each analyte.

β -car	%	0*	8*	16*	24*	32	40	48	56	64	72	80	88	96	100
	μ M	0*	8*	16*	24*	32	40	48	56	64	72	80	88	96	100
lyc	%	100	92	84	76	68	60	52	44	36	28	20	12	4*	0*
	μ M	100	92	84	76	68	60	52	44	36	28	20	12	4*	0*

* the concentrations are lower than the estimated detection limit of the analytes measured individually are marked in italic

2.4. Food extraction

2.4.1. Extraction of B vitamins

Two different extraction protocols were initially tested. A first protocol, referred to as **method A**, is a HPLC protocol optimized by Food GmbH (Jena, Germany) for the extraction of B2. In order to apply this, the cereals were first homogenized, resulting in a small granulated sample. 5 g of the sample was then mixed with 100 ml 0.1 M hydrochloric acid and the resulting solution was boiled for 60 min at 100°C. Following this, the pH of the solution was adjusted to 4 using 2.5 M sodium acetate and 500 mg Taka-diastase was added to it. Next, the mixture was incubated overnight at 40°C. the resulting sample was diluted with a 0.02 M acetic acid solution to 200 ml and the undissolved residues were removed using a folded paper filter. In a last step, the solution was filtered using a PVDF syringe filter (pore size 0.22 μ m) before performing SERS measurements and with a CME syringe filter before the HPLC measurement. Finally, SERS and HPLC measurements were performed. As in the previous cases of B vitamin measurements, the extracts were stored at -4°C until measurement.

A different extraction protocol was tested in order to develop a less time-consuming procedure, referred to as **method B**. This is based on the HPLC extraction protocol optimized for the extraction of B12 and introduced by E. Campos-Gimnez *et al.*³⁰ For this, 25 g granulated cereals were mixed with 100 ml of water at 40°C and 30 g of the suspension of the resulting solution was mixed with 50 mg α -amylase and incubated for 30 min at 40°. Upon this, 50 ml sodium acetate buffer was added and the mixtures were boiled for 30 min at 100°C. Upon

a fast cooling of the resulting solution, this was diluted to 100 mL with water and filtered through a folded paper filter (pore size 8 μm) and a PVDF syringe filter (pore size 0.22 μm). Finally, the extracts were stored at -4°C until SERS and HPLC measurements were performed.

For the further optimization of method B (further referred to as **method C**), the results published by Szterk *et al.*^{105, 106} were used as starting point. That is, solid phase extractions (SPE) cartridges with a reversed phase C_{18} and endcapping (sorbent mass 360 mg) provided by Waters were applied in the next step of optimizing the food extraction procedure. First step consisted in the cartridges' conditioning with 4 ml MeOH and 5 ml 0.025 M phosphate buffer (pH 6). Next, 1 ml extract was added to the column and washed with 2 ml 0.025 M phosphate buffer (pH 6), followed by 8 ml of a MeOH buffer solution (1:1, v/v) in order to elute the analyte and 4 ml MeOH for the removal of the residual components from the solid phase. Finally, the solvent was removed at 30°C and the oily residue was re-dissolved in high purity water. As in the previous case, the extracts were stored at -4°C until the SERS measurements. No further HPLC measurements were performed.

2.4.2. Extraction of carotenoids

The tomato samples were homogenized to obtain a puree. Then 200 mg magnesium bicarbonate, 30 ml methanol/THF solution (1:1, v/v) and 5 g of each pure sample were mixed. The resulting mixture was stirred using an ultra turrax and filtered with a Buchner funnel. The procedure was repeated two times. Finally, the solutions were evaporated to dryness and re-dissolved in the extracting agent. The final sample was measured with both SERS and HPLC. For the SERS measurements a new substrate was used for each extract.

2.5. HPLC measurements

The system used for all the HPLC measurements was a Shimadzu binary gradient system with DGU-20A3R degassing unit, SIL-20AC auto-sampler, CTO-20AC column oven and SPD-20A UV/VIS-fluorescence detector.

For the measurement of the B vitamins the separation was performed on a 250 x 4 mm S-5 μm LiChrospher 60 RP Select B HPLC column and the mobile phase was a combination of sodium acetate buffer (pH 4, 0.05 M - solvent A) and methanol (solvent B) in a ratio of 6:4. The injection volume was 210 μl , the total flow was 0.7 ml/min and the column temperature was 25 $^{\circ}\text{C}$. For the measurement, the extract solutions were initially diluted: the extract obtained using method A was diluted 1:1 and the one obtained according to method B was diluted 1:2 using the mobile phase. The peaks were evaluated via fluorescence spectroscopy and the detection wavelength was set at 468 nm.

For the measurement of the carotenoids the separation was performed on a 250 x 4.6 mm S-5 μm YMC 30 HPLC column and the mobile phase was a combination of 90% methanol (solvent A) and 10% tertiary butyl methyl ether (tBME, solvent B). The injection volume was 50 μl , the total flow was 1.3 ml/min and the column temperature was 29 $^{\circ}\text{C}$. During the measurement a linear gradient was applied up to 55% solvent A and 45% solvent B (45 min). Upon this, another linear gradient up to 45% solvent A and 55% solvent B was applied for 5 min before returning to the starting conditions (90% solvent A), which was applied for 2 min. The peaks were evaluated via fluorescence spectroscopy and the detection wavelength was set at 450 nm and 470 nm respectively.

In both cases an external calibration was performed using four standard solutions and an internal standard for achieving quantification. The limit of quantification (LoQ) determined by the signal to noise ratio was 0.3 $\mu\text{g}/100\text{ g}$ for the B vitamins and 0.03 $\mu\text{g}/\text{ml}$ for the carotenoids.

2.6. Spectroscopic measurements

The extinction spectra of all analytes were recorded with a Jasco V650 diode-array spectrophotometer.

All reference Raman measurements of the powdered analytes were performed using a commercially available WITec confocal Raman system (WITec GmbH, Ulm, Germany) equipped with a 785 nm laser. The laser power at the

surface of the sample was 80 mW and the spectra are recorded within 1 s with 10 accumulations.

For the characterization of the EGNPs the substrates were first incubated in the as prepared solutions of the analyte and then dried with Ar. The SERS measurements were performed using a commercially available WITec confocal Raman system (WITec GmbH, Ulm, Germany) equipped with a 514 nm laser, by focusing the laser beam through a 100× objective (NA 0.8) onto the sample and collecting the scattered light via the same objective. The SERS data was collected as scans consisting of 80 point-measurements (integration time: 0.5 s/point). The laser power used was 20 μ W.

For the characterization of the NSs the substrates were first incubated in the as prepared solutions of the analyte and then dried with Ar. The SERS measurements were performed using a commercially available WITec confocal Raman system (WITec GmbH, Ulm, Germany) equipped with a 488 nm laser, by focusing the laser beam through a 100× objective (NA 0.8) onto the sample and collecting the scattered light via the same objective. The SERS data was collected as scans consisting of 100 point-measurements (integration time: 0.5 s/point). The laser power used was 20 μ W.

For the characterization of the HD-DVDs the substrates were first incubated in the as prepared solutions of the analyte and then dried with Ar. Upon this, the substrate was fixed on a 25×25 metric goniometer with a traveling distance of 40 degrees (LASER 2000, Wessling, Germany) and the angle between the incident beam and the substrate was varied from 0 to 14 degree. The SERS measurements were performed every two degrees using a commercially available WITec confocal Raman system (WITec GmbH, Ulm, Germany) equipped with a 785 nm laser, by focusing the laser beam through a 100× objective (NA 0.75) onto the sample and collecting the scattered light via the same objective. The SERS data was collected as scans consisting of 100 point-measurements (integration time: 0.5 s/point). The laser power used was 1 mW.

For the characterization of the EBL-based substrates a commercially available WITec confocal Raman system (WITec GmbH, Ulm, Germany) equipped with a 488 nm laser use used to focus the laser beam through a 100×

objective (NA 0.8) onto the sample and collect the scattered light via the same objective. The SERS data was collected as scans consisting of 100 point-measurements (integration time: 0.5 s/point). The laser power used was 20 μW . For the measurement of the B vitamin experiment, the substrates were incubated in a Petri dish containing 2.5 ml of the as prepared solutions of the analytes for 10 min and then measured under wet conditions. During the measurements, an optical grating of 600 g/mm was used, resulting in a spectral resolution of $\sim 6\text{ cm}^{-1}$. The laser power at the surface of the sample was 1 mW. For the carotenoid experiment, the substrates were incubated in the analyte solutions for 30 min and then dried in an Ar stream. During the measurements, an optical grating of 1800 g/mm was used resulting in a spectral resolution of $\sim 2\text{ cm}^{-1}$ and the power at the surface of the sample was adjusted to 20 μW . For each measured carotenoid analyte 13 scans were recorded.

2.7. Chemometric-based analysis

For the statistical analysis of the SERS data a free source programming language, GNU R (version 3.0.2)¹⁰⁷ was used and the resulting spectra were then plotted using Origin 8.5. More exactly, for the R-based analysis different methods were applied and are described above.

To conclude on the point-to point reproducibility of the substrates, a background correction of the spectra was performed using the Sensitive Nonlinear Iterative Peak (SNIP)¹⁰⁸ algorithm and then the peak area was estimated using the Simpson's rule.¹⁰⁹ No spectra averaging was performed during this analysis.

For the estimation of all the presented LoD the IUPAC norms were applied, according to which the LoD is equal to the signal of the blank plus three times the standard deviation of the blank. However, before applying this rule, the as-measured SERS spectra were first averaged over 50 point measurements, then the resulting spectra were background corrected using the SNIP¹⁰⁸ algorithm and finally, the Simpson's rule was applied for the peak integration.¹⁰⁹

For the differentiation of the two carotenoids (β -car and lyc) a statistical analysis model was build, consisting in a combination of PCA^{93, 94} and PLSR^{93, 94}.

To build this model the measurements performed on the β -car/lyc mixtures were used as input data as follows: the spectra were first averaged over a 50-point measurement and then, the resulting spectra were wavenumber calibrated and cut to the relevant spectral range of 500-1700 cm^{-1} . The averaging step was performed to compensate for the well-known drawback of SERS data reproducibility for larger scale measurements caused by the chemical binding of the analyte to the substrate.^{110, 111} Upon this, the spectra were background corrected using the SNIP algorithm,¹⁰⁸ spike corrected and normalized for the whole spectral range. After these, a PCA^{93, 94} was performed using different number of components. This was followed by a PLSR^{93, 94} analysis, also using a different number of components and two types of cross-validation. More exactly, for building the training data set all values representing one concentration (carotenoid percentages) were removed (and this was repeated for all different concentrations). In a next step, 1% of the total number of measurements was randomly taken out for training. Finally, the optimal number of principal components for PCA and PLS were decided for, and a model was built using all of the measured data. This model was further applied for the prediction the food composition, by using the SERS spectra measured on the different tomato extracts as test data.

All SERS spectra depicted in this thesis are background corrected.

3. Results and discussion

3.1. Characterization of SERS-active substrates as powerful platform for food analytics

As discussed, a close consideration of the requirements of the particular application is helpful for restricting the range of the available substrates and, in the particular case of this thesis, food analysis based on SERS is performed. Food-relevant analytes such as most vitamins (i.e. vitamins A, E, D, etc.), carotenoids (i.e. β -car and lyc) and some of the food dyes (i.e. BY) are fat-soluble, making water-based colloidal solutions an unpractical choice. Further on, a uniform, high signal intensity of the SERS signal of the target molecule is needed for acquiring a statistically sufficient and reliable database. These databases are further compulsory for attempting to achieve an estimation of the analytes in the food product, which is the final goal of many applications in the food area. Both requirements are most often provided by top-down substrates. Accordingly, different SERS substrates were tested to find the “optimal” combination of uniform, high signal intensity, easy, cost-effective preparation protocol and easy to use substrate. Also, different analytes were used as test molecules in order to achieve a fast overview of the potentials and limitations of these substrates. The chemical structure of these molecules and their UV-vis absorption spectra are depicted in **Figure 2**. Apart from this, these molecules also have different functions in the food products. As already discussed, most of the vitamins and carotenoids are much desired in the food products. This is the case of vitamins A, B2, B12, β -car and lyc. On the other hand, though, different other analytes are added to the food in order to enhance the color of the product even though they might lead to the development of different diseases, including cancer, when ingested in high doses. Such examples are BY or Sudan dyes. More than one of these analytes were considered during the first testing of the substrate in order to get a better overview of the substrates properties, but not all obtained results are introduced below. Instead, in order to achieve a good characterization of the SERS-active substrates tested while performing the measurements, the method of

choice was scanning over different areas of the substrate in order to enable the acquisition of a high spectra database in real-time.

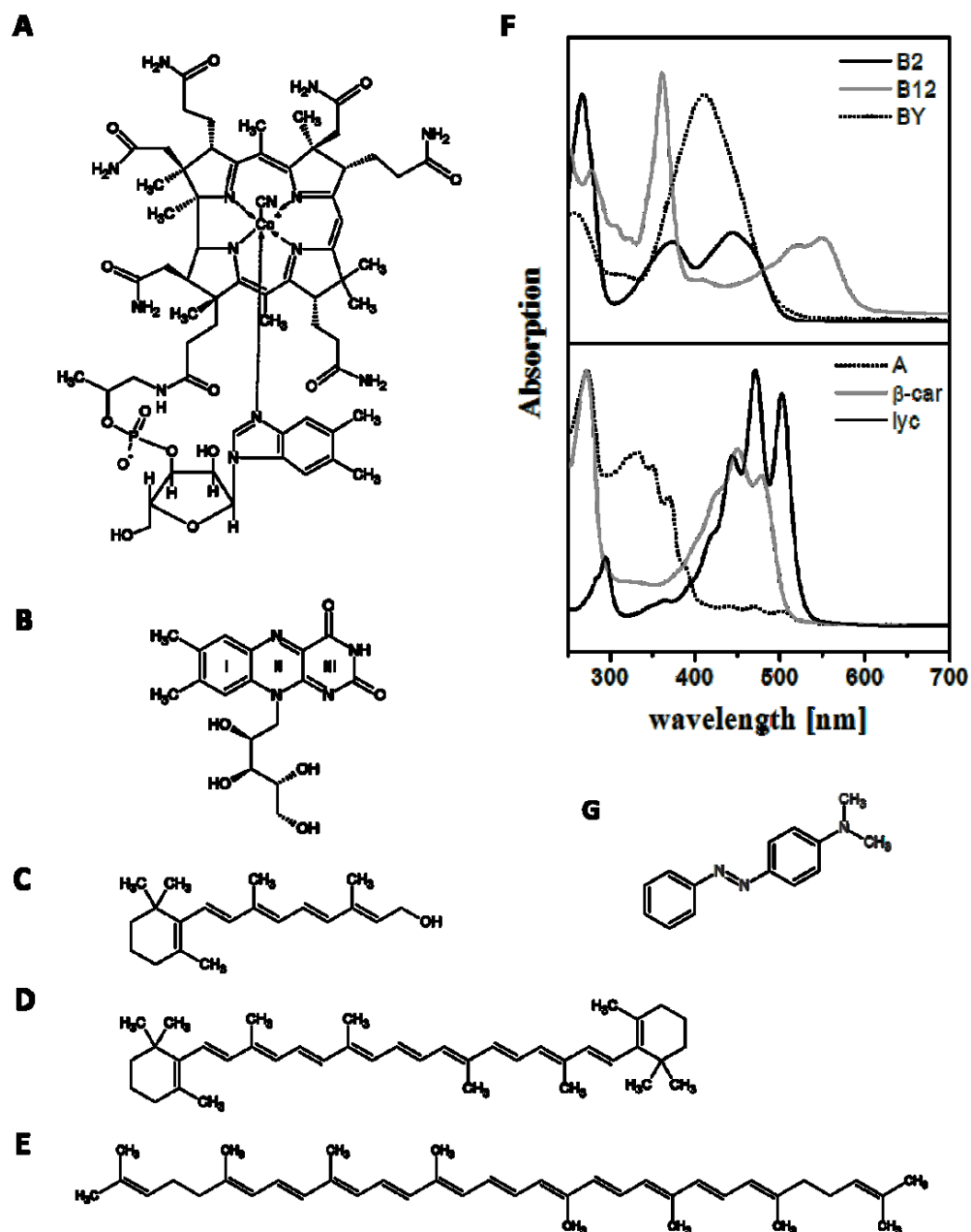


Figure 2 Chemical structure of B12 (A), B2 (B), vitamin A (C), β -car (D), lyc (E), BY (G) and extinction spectra of all named molecules (F).

Upon this, individual scans were analyzed to decide on the point-to-point reproducibility of the substrates. This was performed for each of the substrates

considered. By combining this information with information related to the preparation protocol reproducibility and price-availability information a comparison of the different substrates was achieved. Further on, based on the preparation protocol reproducibility it was possible to achieve indirect information about the shelf-life of the substrates. Finally, by analyzing all these information together it was possible to decide on the “best” applications and data analysis procedure for the investigated substrates and to choose the “best-suited” substrate for food applications.

3.1.1. Enzymatically generated silver nanoparticles (EGNPs)

EGNPs are relatively cost effective (estimated price: 5 euro/substrate¹) and easy to prepare bottom-up SERS-active substrates. That is because their assembling requires only a few chemicals (among which PBS, single-stranded biotinylated DNA, HRP and others, as described in the *Materials and methods* section), a clean, stable environment and a few different experimental steps. Their drawback, however, consists in the short shelf-lifetime, as the substrates need to be prepared short before the measurement and the full protocol is rather time consuming (around 3 hours). Additional to this, the development of reproducible EGNPs is dependent on assuring stable lab conditions (*i.e.* temperature and humidity) due to the nature of the interactions between the chemicals. The SEM image of the resulting SERS-active substrates is depicted in **Figure 3** and present a “desert-rose like” structure and a broad-band absorption covering the entire visible spectral range as already introduced in the study of K. K. Hering *et al.*¹⁰³

¹ Rough estimation of the production price (as given by the technology requirements). This is not an estimation of a market price.

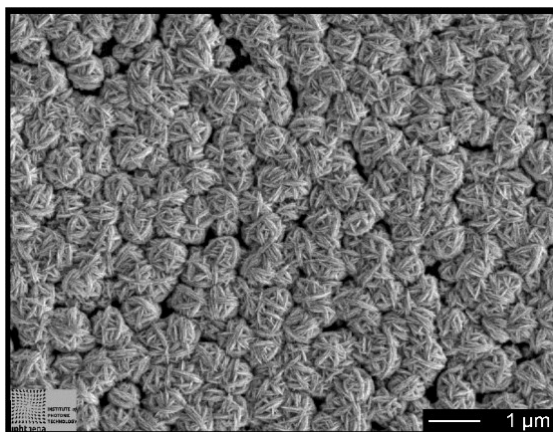


Figure 3 SEM image of the measurement field of the EGNPs.

The potential of the EGNP substrates for the detection of food relevant analytes was tested and is exemplified for the detection of vitamin B2. This was performed by using a 10 μM B2 solution. For the measurement, the EGNPs were incubated in the analyte solution and then measured by applying a 514 nm laser. As observed from the extinction profile of B2 (see **Figure 2**), a gain from the resonance measurements conditions was expected by using the named laser line as an excitation source. The measured SERS spectrum is depicted in **Figure 4** together with the spectrum of the background of the EGNP substrate and the Raman spectrum of B2 measured on the powdered analyte by applying a 785 nm laser source for excitation. A good identification of the analyte can be achieved by using EGNP substrates as observed by the presence of the fingerprint bands centered at 1340 cm^{-1} (assigned to the in-plane ring bending vibrations of aromatic rings II and III)¹¹² and 1155 cm^{-1} (assigned to the in-plane ring bending vibrations of aromatic rings II and III, NH bending of ring III and twisting of CH in the aliphatic chain).¹¹² Additionally, the low intensity bands centered at 1626 cm^{-1} (assigned to the in-plane ring bending vibration of ring III as well as the N–H and C=O stretching vibrations)¹¹² and 1081 cm^{-1} (assigned to in-plane ring III bending vibrations and the bending vibrations of C-H in the aliphatic chain)¹¹² in the Raman spectrum become better defined under SERS measurement conditions. This might be further correlated to the binding of the molecule to the substrate via the nitrogen/oxygen atoms present in the rings II and III.

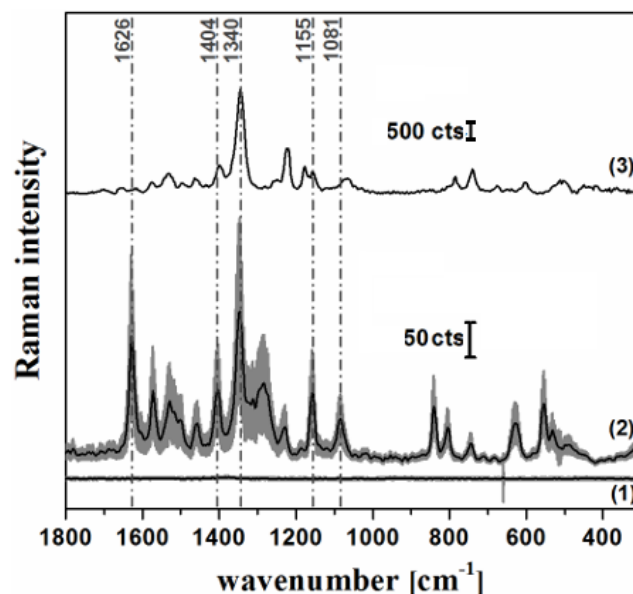


Figure 4 SERS spectra of the EGNPs background (1) and of 10 μM B2 measured on the EGNP substrate (2). The Raman spectrum measured on powdered B2 (3) and used as a reference is also depicted.

Next, different scans were performed on the surface of the substrate to assess the point-to-point reproducibility. For this, the EGNP substrate was incubated in a 10 μM B2 analyte solution, dried and measured. Finally, the spectral range corresponding to the band centered at 1081 cm^{-1} was used for peak integration. **Figure 5** depicts the results in the form of point-by-point reproducibility within one scan. Moreover, the calculated relative standard deviation (RSD) by applying the EGNP substrate is 17%. Considering that the “ideal” SERS active substrate for food applications should not present more than 20% deviation over the surface of the substrate,^{58, 61} the EGNPs were found to have a good point-by-point reproducibility.

Considering all discussed aspects, the EGNPs are a cost effective substrate that presents a good point-to-point reproducibility and a broad absorption band, but that need to be freshly prepared before the measurement. Moreover, their preparation requires stable lab conditions in order to achieve batch-to-batch reproducibility. Further on, the background of the as prepared substrates (**Figure 6**) presents strong peaks centered at 1391 cm^{-1} (assigned to the combined C–C stretching and C–H bending vibrations of p-benzoquinone)¹⁰⁰, 1019 cm^{-1} (assigned

to the C–C stretching vibration of the hydroquinone – p-benzoquinone complex)¹⁰⁰, 945 cm⁻¹ (assigned to the combined bending C–C and C–H vibrations of p-benzoquinone)¹⁰⁰, 800 cm⁻¹ (assigned to the out of plane vibration of hydroquinone)¹⁰⁰. Additional to this, a further contribution to the substrates background is also expected from the citrate buffer used for the silver deposition. More exactly, a Raman mode centered at 1400 cm⁻¹ (assigned to the COO stretching vibration)¹⁰⁰ and 945 cm⁻¹ (assigned to the C–C stretching vibration)¹⁰⁰ are expected in the SERS spectrum of the background. The presence of these bands in the background spectrum hinders the achievement of a low LoD for the detection of different molecules, decreasing the application range of the EGNP substrates. Accordingly, EGNP SERS-active substrates were not considered the best-suited substrates for the development of SERS-based applications towards food analysis.

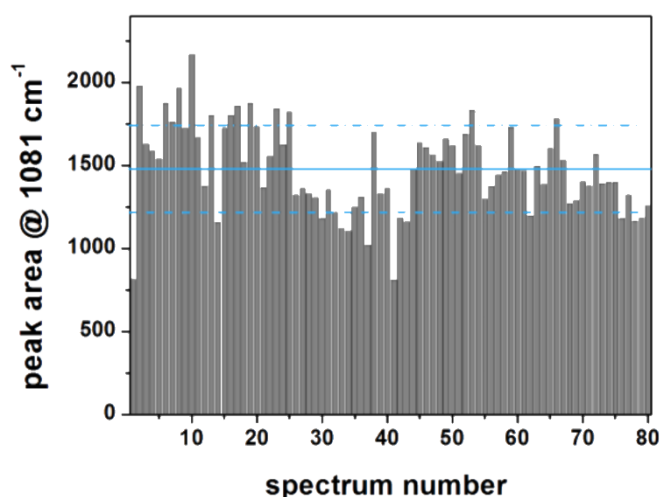


Figure 5 Point-to-point stability of the 1081 cm⁻¹ B2 peak within a single scan on a EGNP substrate that has been prior incubated in 10 μM B2 solution.

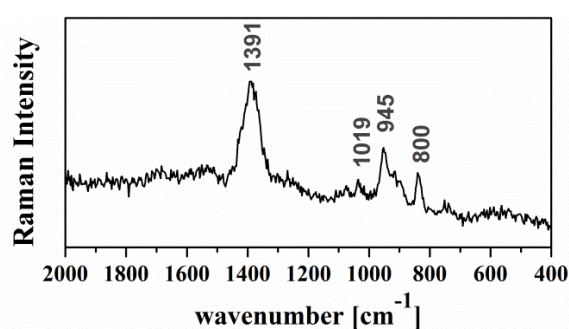


Figure 6 SERS spectrum of the background of EGNP substrates.

3.1.2. Nano-sponges (NSs)

NS substrates are produced via a combination of top-down and bottom-up approaches, resulting in a relatively cost effective substrate (estimated price: 5 euro/substrate^{II}). The first step for preparing the NSs consisted in preparing a silicon wafer coated with silica (SiO_2/Si) by means of nanoimprint lithography. Then an Ag layer and an Au layer are deposited on top. Following this, an annealing process leads to dewetting and to the formation of mixed Au/Ag nanoparticles. Finally, the silver is removed, resulting in Au nano-sponge-like structures (Au NS). Further on, by performing the additional steps described in the *Methods* section an additional layer of Ag can be deposited on the Au NS, resulting in Ag/Au nano-sponge-like structures (Ag/Au NS). Both substrates were structurally characterized previously and a detailed description of the Au NSs can be found in the publications of D. Wang *et al.*^{101, 102} The Ag/Au NSs structural characterization and spectroscopically behavior is comprehensively investigated by Y. Yan *et al.*¹¹³ More exactly, the extinction spectrum of the Au NS presents a broad band covering the spectral range 500-1500 nm and centered around 1100 nm. As compared to this, the extinction spectrum of the samples containing Ag, Ag/Au NS presents a sharp peak centered around 860 nm and two lower intensity peaks centered around 600 nm and 300 nm.

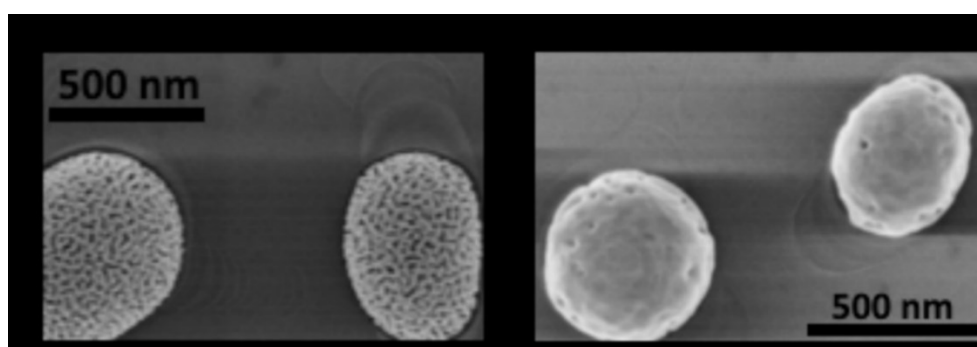


Figure 7 SEM images of the measurement fields of the Au NS (A) and of the Ag/Au NS

^{II} Rough estimation of the production price (as given by the technology requirements). Moreover, it only stands for the production of an entire wafer consisting of 100 chips/wafer. This is not an estimation of a market price.

A SEM image of the two different substrates can be observed in **Figure 7**. As depicted, the addition of Ag to the Au NS seems to lead to the closing of the pores present in the Au NS, without affecting the overall size of the mesoparticles. However, the presence of the Ag layer strongly influences the shelf-life of the substrates. More exactly, the Au NS can easily be stored upon preparation until the date of the measurements. This is not valid for the Ag/Au NSs. Instead, the Ag layers would, ideally, be prepared close to the SERS measurements.

The NS substrates were tested for the detection of butter yellow (BY), which is a dye used in the food industry for achieving a brighter yellow color of different products. A 488 nm excitation source was used for these measurements. By analyzing **Figure 2**, it is expected to have a contribution from the analytes' resonance measurement conditions by applying the 488 nm excitation source. The obtained SERS spectra are depicted in **Figure 8** together with the reference Raman spectrum of the molecule measured on a powdered BY using a 785 nm excitation source. As in the previous case, a good identification of the molecule can be achieved by SERS. By closely analyzing the spectra, it can be observed that in the case of the Au NS selective enhancement was achieved for the bands centered at 1615 cm^{-1} (assigned to C=C stretching vibration)^{114, 115} and 1590 cm^{-1} (ascribed to the benzene ring vibration)¹¹⁴. Generally, based on the surface selection rules, the enhancement of the in-plane ring vibrations might indicate a perpendicular orientation of the molecule on the metallic surface.¹¹⁶ Further bands can be observed centered at 1486 cm^{-1} (assigned to the benzene ring vibration)¹¹⁴, 1410 cm^{-1} (assigned to the stretching vibration of N=N and C-N bands)¹¹⁵ and 1364 cm^{-1} (assigned to the stretching vibration of C-N and C-C bands)¹¹⁵. As compared to the first case, for the Ag/Au NS a higher signal intensity was achieved for the bands centered at 1410 cm^{-1} and 1130 cm^{-1} (assigned to the stretching vibration of C-N and C-C bands).¹¹⁵ This might be related to the interaction of the molecule with the substrate via the nitrogen atoms.¹¹⁷ For more detailed insights into the molecule-metal interaction a full vibrational analysis of BY has to be performed and it is beyond the purpose of the present study. Further on, in the case of the Ag/Au NS a higher signal intensity of the analytes Raman signal was achieved as compared to the Au NS, as observed from the spectra in **Figure 8**.

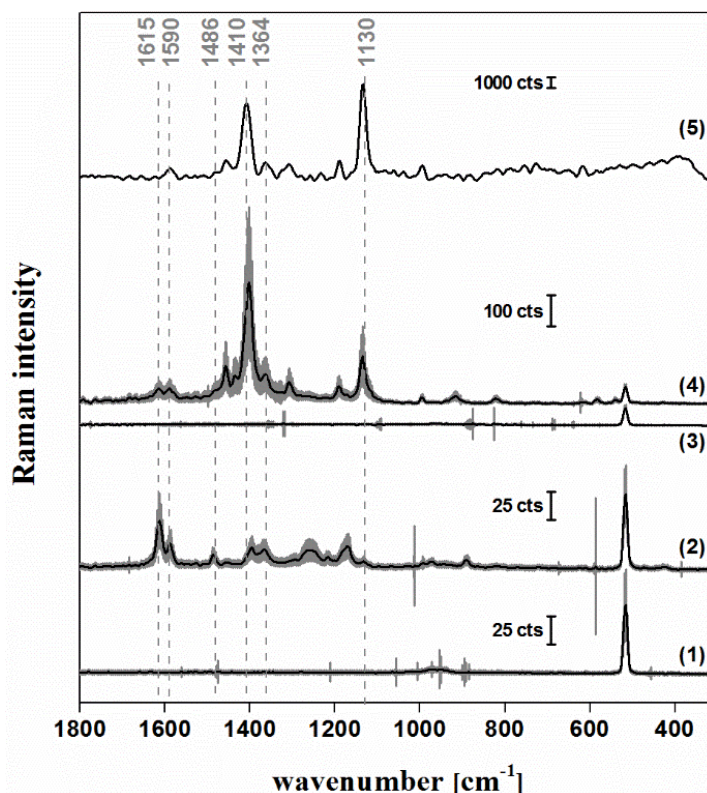


Figure 8 The SERS spectra depicts the Au NS substrates background signal (1), the 100 μM BY SERS measured on a Au NS substrate (2), the Ag/Au NS substrates background signal (3), the 100 μM BY SERS measured on a Ag/Au NS substrate (4) and the Raman spectrum measured on powdered BY and used as a reference (5).

The spectra in **Figure 8** reveal the presence of the Si peak centered at 515 cm^{-1} in both the spectra of the substrates' background and the spectra of BY. This is explained by the usage of the SiO_2/Si under-substrate during the preparation. In order to investigate whether this peak could be further used as an internal standard the peak area of this band was calculated and the plots of the variation of the peak area within one scan (consisting of 100 point measurements) are depicted in **Figure 9**. Here the peak area stability is presented for the case of the measurement performed upon incubation of the substrate in the BY analyte solution. By analysing the stability of the 515 cm^{-1} peak area within one single scan RSD values of 10% and 14% were obtained for the measurement of Au NS and Ag/Au NS respectively. Accordingly, a good point-to-point stability of the Si peak is provided by the two substrates. Still, considering that the substrate preparation protocol results in a non-uniform coverage of the SiO_2/Si wafer with nanosponge-like structures^{102, 113} (**Figure 7**), the Si peak could only be used as an internal

standard if its intensity would fluctuate as a function of the presence of the nanosponge-like structures. This is, however, not the case. These led to the conclusion that the Si band would not be an ideal internal standard at this point of the substrate development. Apart from this, it is also expected that an increase in the overall coverage of the wafer with nano-sponge-like structures and an increase in their ordering on the substrate might lead to a better SERS substrate.

Further on, to investigate the stability of the SERS signal of the analyte by applying the NS substrates, the peak centered at 1615 cm^{-1} (assigned to C=C stretching vibration)^{114, 115} and the peak centered at 1130 cm^{-1} (assigned to the stretching vibration of C–N and C–C bands)¹¹⁵ were also analyzed for the case of the Au NS and the Ag/Au NS respectively. All obtained results are depicted in **Figure 9**. In the case of the Au NS a RSD of 16% was achieved, while for the Ag/Au NS a RSD of 70% was obtained. Considering that the “ideal” SERS active substrate for food applications should not present more than 20% deviation over the surface of the substrate,^{58, 61} it was concluded that the Ag/Au NS would need much improvement before being used for an application. Regarding the Au NS, the value of the obtained RSD proves that the point-to-point reproducibility of the substrate is very high. However, by analyzing **Figure 9** and keeping in mind that the concentration of the measured analyte was high (100 μM) it was concluded that the NS substrate is not the best choice for being used for an application. Moreover, as presented in the *Materials and methods* section, the two substrates were prepared according to the same protocol (until the Ag deposition step) and resulted in substrates having a very different point-to-point reproducibility. As the Ag deposition step does not dislocate the sponges, the results in **Figure 9** provide important information regarding the relatively low batch-to-batch reproducibility of the substrates. However, one should keep in mind that this is just an expected result, as the morphology of the Au NS is different from the Ag/AU NSs. Accordingly, the NS SERS-active substrates were not considered best-suited substrates for the development of SERS-based applications towards food analysis.

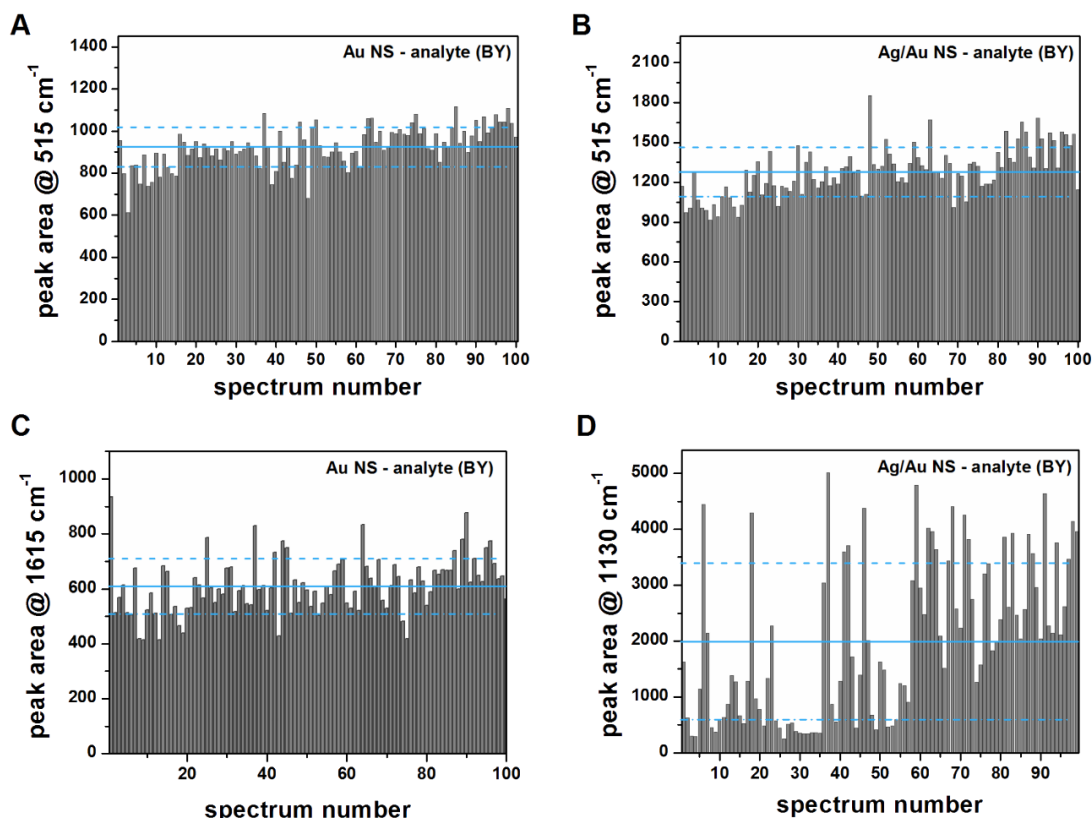


Figure 9 Pont-to-point stability of the 515 cm⁻¹ Si peak within a single scan measured on the Au NS (A) and Ag/Au NS (B); and pont-to-point stability of the 1130 and 1615 cm⁻¹ BY peaks within a single scan on the Au NS (C) and Ag/Au NS (D) respectively. All measurements were performed using a 488 nm laser.

3.1.3. HD-DVD-based substrates

HD-DVD-based SERS substrates are produced starting from a commercially available optical storage device (HD-DVD) according to the protocol described in the *Materials and methods* section. Briefly, upon opening the HD-DVD and cleaning it, a 30 nm layer of Au was deposited via sputtering, resulting in the structure presented in the SEM picture depicted in **Figure 10**. Considering the price of an HD-DVD (\$0.90 to \$1.50 per piece^{III}) and the additional prices for cleaning and Au layer sputtering the final SERS substrate is at the same time cost effective, easy and fast to prepare. All these make it a good candidate for applications.

^{III} Market price

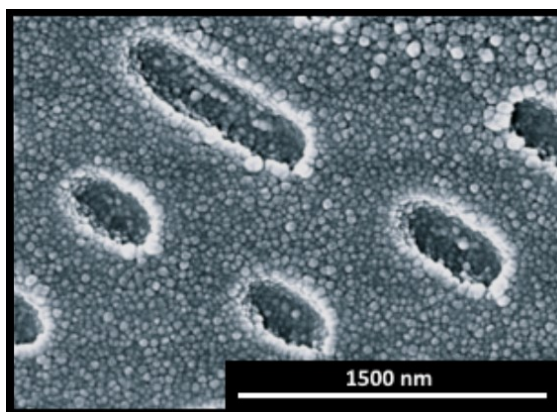


Figure 10 SEM image of the HD-DVD-based substrate. Adapted from Ref. 111¹¹⁹ with permission from The Royal Society of Chemistry.

The first step consisted in the structural characterization of the obtained HD-DVD-based substrates. It was found that due to the information pre-encrypted in the commercially available optical storage devices (*i.e.* movies, music, etc), the templates of the resulting SERS-active substrates present a pit-like structure consisting of nanostructures having a 250 nm width, a 35-80 nm depth and varying lengths in the range of 200-1000 nm. These pits are arranged in concentric rings having a periodicity of 400 nm.^{118, 119} Further on, these structures are still present upon Au sputtering and provide the resulting SERS substrates with an angular dependence of the SERS signals upon illumination from an oblique incident angle on the substrate (see A.I. Radu *et al.*¹¹⁹ for further information about the plasmonic properties of the substrates). More exactly, the reflection spectrum of the substrates was calculated by Ye.Ye. Ussembayev using the commercially available finite-element modelling (FEM) package provided with COMSOL Multiphysics 4.3a. For this, a single 3D unit cell confining the reconstructed geometry of the encoding pit (250 nm width, 60 nm depth and 900 nm length) was used in combination with Floquet periodic boundary conditions in the x- and y-directions. Furthermore, to account for the absorption of the electromagnetic field components reflected or scattered from the boundaries perfectly matched layers were set in z direction (the direction of light propagation under normal incidence). The obtained reflection spectrum features two resonance minima (not presented here) which correspond to the short-range SPP (SR-SPP – the first minimum at

smaller angle) and the long-range surface plasmon polaritons (LR-SPP – the second one at larger angle) modes. This is, however only valid for the case of a thin metal layer. Furthermore, according to the simulation results, the substrates LSPR can be induced with wavelengths varying between 500-600 nm.

To experimentally test the existence of an angular dependency of the SERS signals upon illumination from an oblique incident angle on the substrate, two different molecules were chosen (β -car and vitamin A) and angular dependent measurements were performed (see *Materials and methods* section for details regarding the measurements). A 785 nm laser was used as excitation source during the SERS measurements and no resonance contribution was observed (as expected upon analyzing **Figure 2**). Further on, during the experiments, 100-point measurement scans of the substrate were performed line-wise, parallel to the length of the encoded pit structure and a 100x (0.75NA). The obtained SERS spectra are plotted in **Figure 11A-B** and depict a dependence of the measured SERS signal to the angle of incidence.

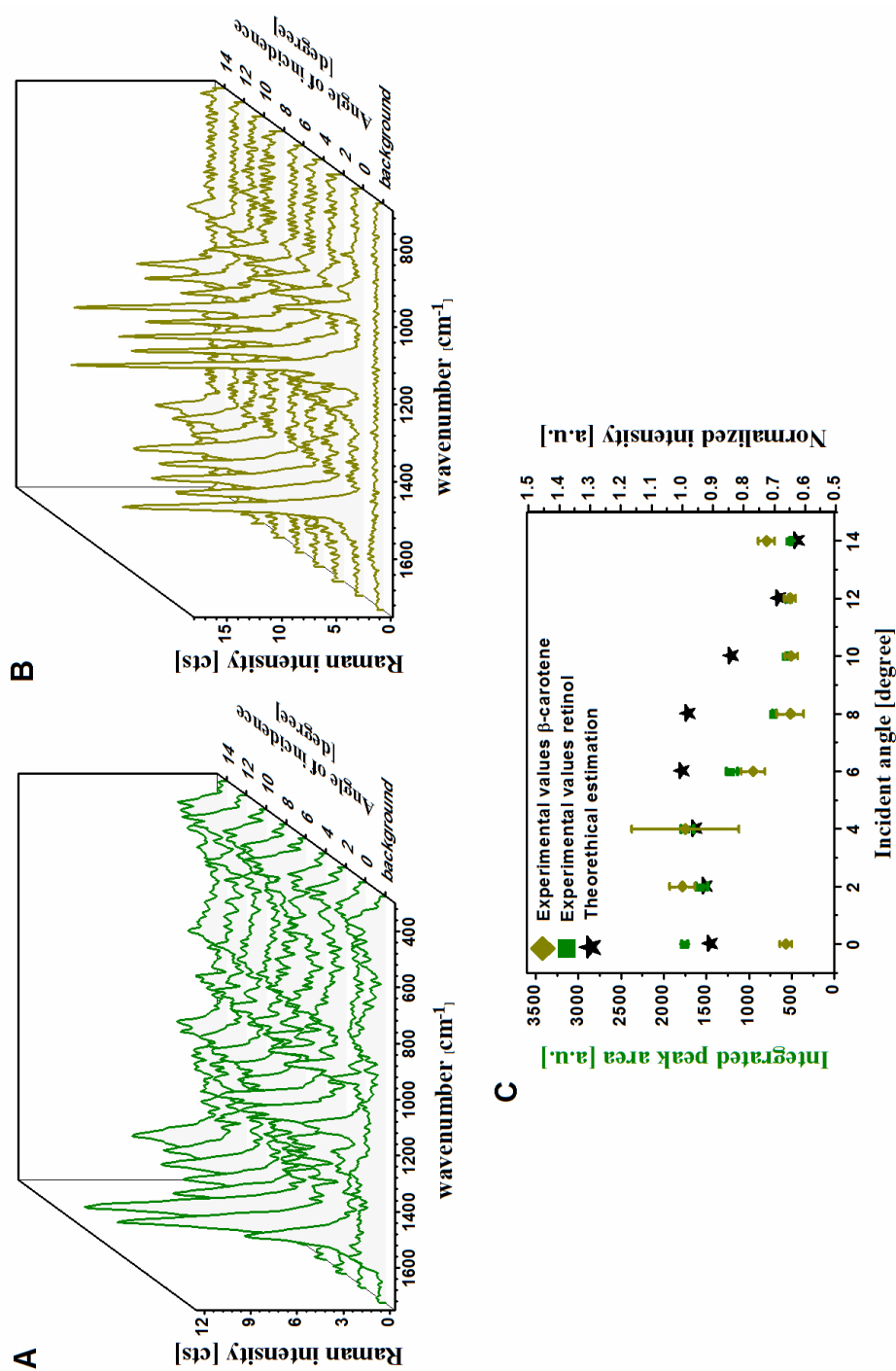


Figure 11 SERS spectra of 1 mM vitamin A measured for different angles of incidence (A), SERS spectra of 1 mM β -carotene measured for different angles of incidence (B) and peak area of the 1569 cm⁻¹ vitamin A band, the 1533 cm⁻¹ β -car band and theoretical calculation results as function of the angle of incidence between the laser beam and the substrate (C). The plotted measured data include the standard error of the mean. Adapted from Ref. 111¹¹⁹ with permission from The Royal Society of Chemistry.

For a better visualization of the results plotted in **Figure 11A-B**, the peak area of the band centered at 1584 cm^{-1} in the spectra of vitamin A (assigned to the C=C stretching vibrations of the molecules polyene chain)^{120, 121} and the band centered at 1521 cm^{-1} in the spectra of β -car (also assigned to the C=C stretching vibrations of the polyene chain)¹²² were calculated. The obtained results are depicted in **Figure 11C** together with the results of the numerical simulations for the same dependency. As observed in this figure, a good agreement was obtained between the experimental and theoretical results considering that the FEM was performed starting from a single, idealized 3D structure of the pit (having fixed dimensions of 250 nm width, 60 nm depth, 900 nm length and 400 nm periodicity), that was considered to reproduce the infinite array of the encoding pits.¹¹⁹ By applying this assumption in the FEM, the simulated SERS template was highly ordered and the afferent dependency of the SERS signal to the angle of incidence of the laser beam (depicted in **Figure 11C**) predicted that a 6° incident angle would be the best detection scheme. As compared to this, the actual optical storage device had fluctuating pit dimensions and additional small variations in the Au spotted grain sizes, as observed in **Figure 10**. Due to these, variations from the theoretical model were observed during the measurements, while the existence of the angular dependency was successfully confirmed. Moreover, based on the angle dependent SERS measurements, a incident angle 4° was chosen as the optimal measurements condition for applying this substrate.

Next, as in the case of each of the substrates considered before, the point-to-point stability within one scan was investigated. For this, 50-point measurement of the substrate upon immersion in vitamin A were measured and the obtained spectra are depicted in **Figure 12A**. As observed, the identification of the molecule can be achieved for 1 mM solutions. Further on, the peak centered at 1584 cm^{-1} (assigned to the C=C stretching vibrations of the molecules polyene chain)¹²¹ was used for peak area calculation and the results are plotted in **Figure 12B**. The obtained RSD value was 9% for 4° incident angle. During these measurements the SERS scans were performed line-wise, parallel to the length of the encoded pit structure and a 100x (0.75NA). Accordingly, a high non-uniformity of the pit length within the substrate and a high non-uniformity of the distance between two

pits was experienced during the measurements. Further on, this is due to the usage of a commercially available (pre-encrypted) optical storage device during the first tests. More exactly, depending on the exact information on the HD-DVD (*i.e.* music, movie, etc) the pit length and density fluctuates so as to provide the “targeted” market with a competitive product. Still, a more symmetrical pit structure could be defined and this would lead to a decreased RSD value. Accordingly, the tested, commercially available, pre-encrypted HD-DVD substrates have the potential of being well-suited for food applications, due to the simplicity of the substrate, it’s preparation and price. Moreover, upon development of a more symmetrical pit structure and it’s imprinting the HD-DVD-based substrate technology could be tested for easy and price efficient SERs-based food analysis.

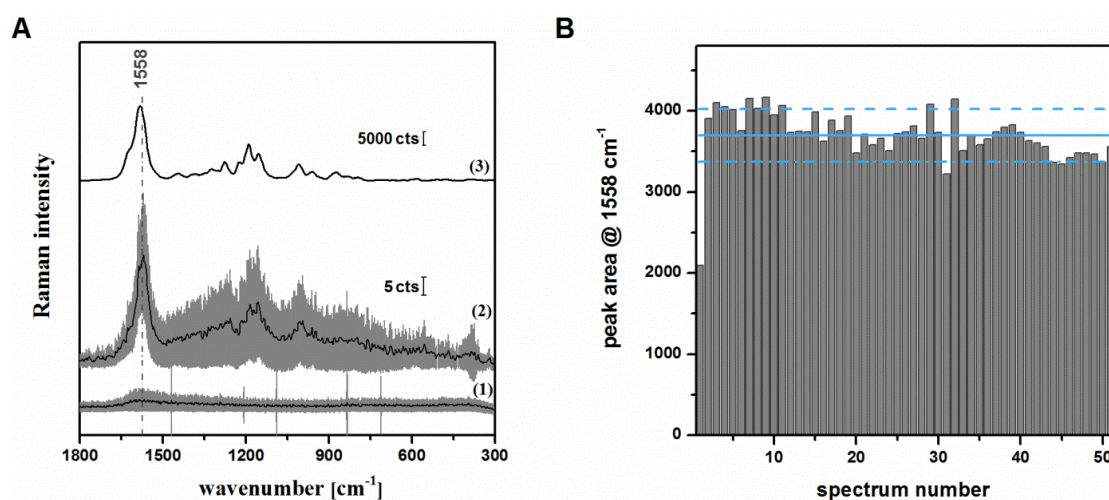


Figure 12 The SERS spectrum of the HD-DVDs background (1,A), the vitamin A SERS spectrum measured at 4° incident angle (2,A) and the Raman spectrum measured on powdered vitamin A (3,A) and used as reference. Point-to-point stability of the 1558 cm^{-1} vitamin A peak area within a single scan on a substrate that has been prior incubated in 1 mM vit A solution (B).

3.1.4. EBL-based substrates

EBL substrates are produced via a top-down approach, resulting in a relatively costly substrate (estimated price: 20 euro/substrate^{IV}). Basically, a fused silica wafer is structured by the use of EBL in order to obtain SERS-active substrates having the geometry depicted in the SEM image in **Figure 13**. The depths of these structures are around 100 nm, the thickness of the applied Ag layer is 40 nm and two different periodicities were tested: 250 nm and 436 nm. Due to the periodicity difference the plasmonic behavior of the two substrates is different. More exactly, for the case of the two substrate having periodicities of 250 and 436 nm a plasmon resonance occurs for an excitation wavelength around 460 nm¹²³ and 500 nm⁷⁶ respectively. Further on, as mentioned in the *Methods* section, the EBL-templates of the substrates can be prepared and stored for the needed time, while the 40 nm thick Ag layer should only be deposited (*i.e.* by thermal evaporation) short before the measurement. Accordingly, this preparation protocol leads to highly ordered and reproducible SERS-active templates having a very long shelf life.

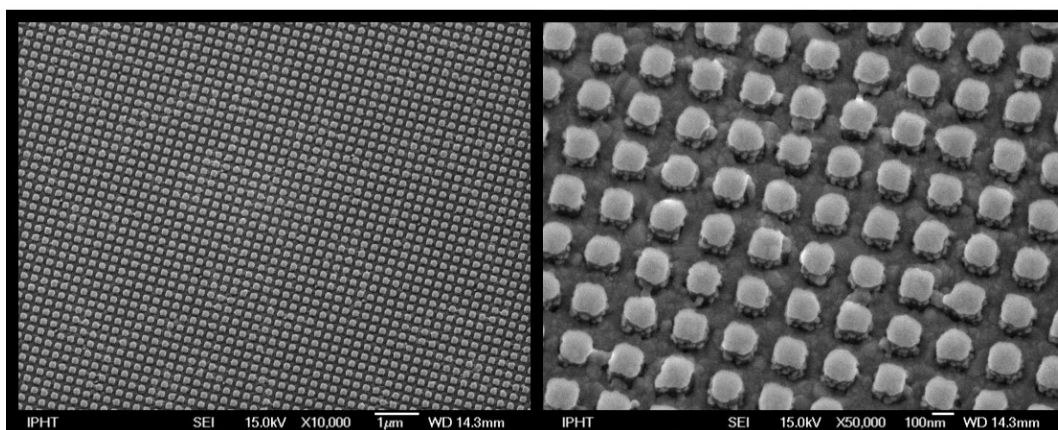


Figure 13 SEM images of the measurement fields of the EBL-based substrates. Adapted from Ref. 116¹²⁴ with permission from The Royal Society of Chemistry.

^{IV} Rough estimation of the production price (as given by the technology requirements). Moreover, it only stands for the production of an entire wafer consisting of 140 chips/wafer. This is not an estimation of a market price.

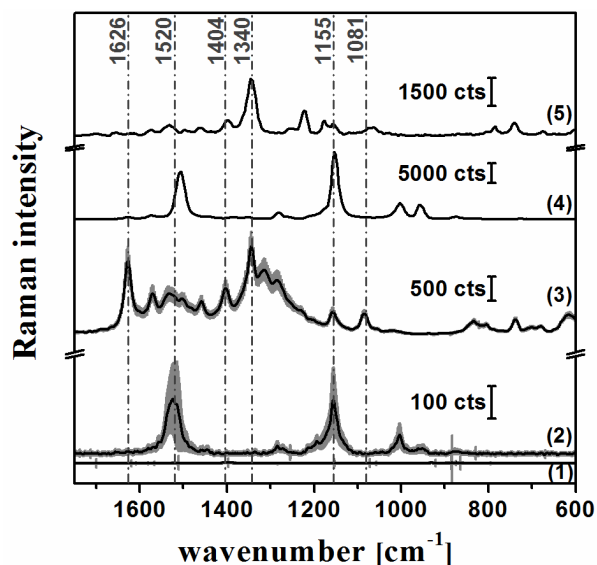


Figure 14 The SERS spectra of the EBL-based substrates background (1,A), the 100 μM lyc (2,A) and 1 μM B2 (3,A). Raman spectra measured on powdered lyc (4,A) and B2 (4,A), used as a reference.

The structural characterization of the substrates was comprehensively investigated by U. Huebner *et al.*^{76, 104, 123} and their spectroscopic behavior towards the detection of vitamin B2 and lyc is introduced here. Through these measurement a 488 nm laser was applied as excitation source. By doing so, a gain from the resonance measurements conditions was expected in the case of B2 and lyc as observed by analyzing their extinction profiles (**Figure 2**). The measured SERS spectra are presented in **Figure 14** together with the spectra of the background of the substrate and the Raman spectra of the analytes measured on the powdered substances by applying a 785 nm laser source for excitation. As observed, a good identification of both analytes can be achieved by using the SERS-active substrates. In the case of lyc, the bands centered at 1155 cm^{-1} (assigned to C-C stretching vibrations of the polyene chain of the two molecules^{122, 125}) and 1520 cm^{-1} (assigned to C=C in-phase stretching of the polyene chain of the two molecules^{122, 125}) can be detected in both the SERS spectrum and the Raman spectrum of the analyte measured on the powdered substance. Same is valid for the case of the bands centered at 1626 cm^{-1} (and assigned to the in-plane ring bending vibration of ring III as well as N-H and C=O stretching vibrations, all belonging to ring III¹¹²), 1340 cm^{-1} (assigned to assigned to the in-plane ring bending vibrations of aromatic rings II and III¹¹²) and 1081 cm^{-1} (assigned to the convoluted

contribution of the in-plane ring III bending vibration and the bending vibration of the aliphatic C-H chain¹¹²) for the case of B2

In a next step, the point-by-point reproducibility of the measurements performed with these substrates was analyzed. As in the previous cases, in order to do this, different scans consisting of 100 point measurements were performed on the surface of the substrate. Then, the spectral range corresponding to the band centered at 1626 cm^{-1} for the case of B2 and the one centered at 1520 cm^{-1} for the case of lyc were used for peak area calculation. **Figure 15** depicts the point-by-point reproducibility within one scan. For the detection of lyc a RSD of 20% was achieved (substrate periodicity: 436 nm), while for the detection of B2 a RSD of 10% was achieved (substrate periodicity: 250 nm). When comparing these results one should consider the different measurement conditions: the lyc measurements were performed under dried conditions by using a 100x objective (NA 0.9) while for the case of the B2 measurements wet conditions and a 10x objective (NA 0.25) were used. As often discussed before, the choice of the measurement procedure was done in order to account for achievement of a good analyte identification and not in just for the purpose of comparing substrates according to a pre-defined scheme. Accordingly, the obtained RSDs are used together to conclude on the EBL-based substrate preparation protocol rather than compared to one-another. Furthermore, considering that the “ideal” SERS active substrate for food applications should not present more than 20% deviation over the surface of the substrate,^{58, 61} it was concluded that the EBL-based substrate fulfill this requirement. Moreover, if possible for the individual application, the performance of the measurements under wet conditions would lead to a higher point-to-point reproducibility. In addition to this, the substrate provides for a long shelf-life as long as the Ag layer is deposited short before the measurements. Accordingly, the tested substrate can be considered for the SERS-based food applications.

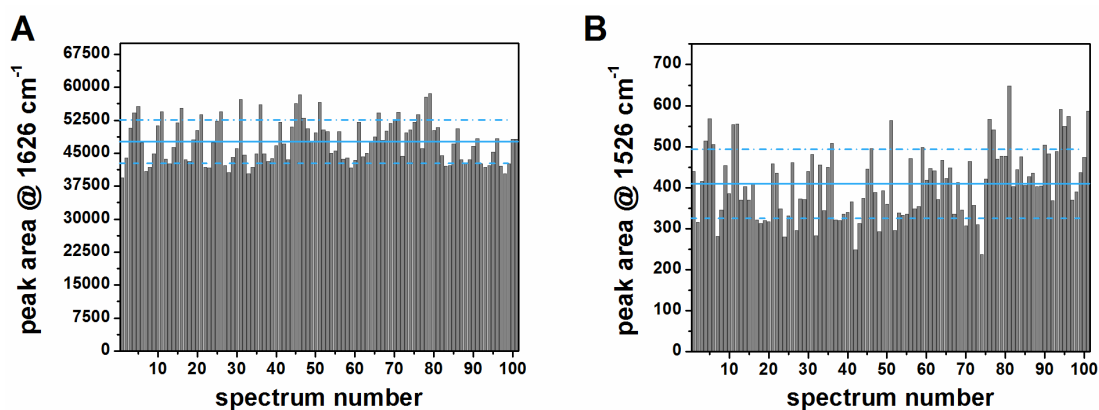


Figure 15 Pont-to-point stability of the 1626 cm^{-1} B2 peak area within a single scan on a 250 nm periodicity EBL-based substrate (A) and of the 1520 cm^{-1} lyc peak area within a single scan on a 463 nm periodicity EBL-based substrate (B).

All above discussed substrates and their characteristics are summarized in **Table 4** for an easy visualization of their strengths and weaknesses. Among the investigated substrates the EGNPs and the NSs present structures of around 700 nm, but having either sharp needles (EGNPs) or nanosponges-like structure (NSs), while the ones based on HD-DVDs and the EBL have smaller nanostructures (see **Table 4**). This is further related to the different laser wavelengths used to excite the plasmon resonances of the substrates (also provided in **Table 4**). Further on, all introduced substrates are feasible for the measurement of fat-soluble analytes as well as water soluble analytes and their preparation protocol is price efficient as compared to other commercially available SERS substrates.^{126, 127} However, the complexity of the preparation protocol varies a lot from opening, cleaning and sputtering a commercially available optical storage device (HD-DVD-based substrate) to EBL lithography (EBL-based substrates) or an DNA-based chemical preparation procedure (EGNPs). Nevertheless, before concluding on this topic, it is important to connect it to the substrate-storage feasibility. Depending on the enhancing metal used for the substrates (Au or Ag), an estimation of the storage possibility can be made (see **Table 4**). Still, as well known, the substrates using Ag as the enhancing material have a short shelf-life

due to oxidation and, in an ideal situation the Ag layer would only be applied short before the SERS measurement. In this case, some of the substrate preparation steps are not required to be done by the person performing the SERS measurements. Instead, the preparation protocol can be stopped at a point and the substrates can be stored for as long as needed. Accordingly, a new classification of the studied SERS-active substrates can be done based on the amount of work and time required by the operator of the SERS experiment: direct application of the substrate without any additional preparation steps (Au NS), simple Au/Ag layer deposition required short before measurements (HD-DVD, EBL based substrates and Ag/Au NSs), close to full preparation procedure required short before the measurements (EGNPs). Each of the tested substrates, with the exception of the EGNPs, can be stored for the required time if the means for applying the required Ag layer are available short before the measurement (see the *Methods* section for more details). Finally, all substrates using Au alone can be prepared, stored for the needed time and directly applied for the measurement. It should also be emphasized that in the case of HD-DVD and EBL-based substrates, both Ag and Au can be easily used and depending on this a different outcome regarding shelf-life and price would be expected.

Regarding the point-to-point reproducibility of the SERS signal detection, EGNPs and NS-based substrates do not have a well-structured surface. Even so, the coverage of the EGNPs is very uniform as proved by the obtained RSD value. HD-DVD-based substrates present a relatively defined periodicity, but this is dependent on the information encrypted on the DVD template (*i.e.* exact movie, music, or other information). However, as already discussed, the substrate can be developed into one having a higher periodicity by mathematically defining the encryption information. Finally, the EBL-based substrates present a highly structured, reliable and reproducible periodicity.

Upon analyzing all information summarized in **Table 4** and discussed above, the EBL-based substrates were chosen for the testing and development of SERS-based food analysis. However, based on the results presented in this chapter the best-suited SERS-active substrate would provide a combination of the positive feature of HD-DVD and EBL-based substrates: highly periodic surface that provides a high point-to-point signal detection reproducibility and can be applied

for dry and wet measurements of water and fat-soluble analytes. Additionally, by imprinting the structures specific for the EBL-based substrates on the PC (polycarbonate) material used for HD-DVD production the preparation price would significantly decrease.

Table 4 Summary of the characteristics of the SERS-active substrates investigated.

	Au NS		Au/Ag NS		EGNPs	HD-DVDs	EBL substrates
	silicone band 515 cm ⁻¹	analyte band 1130 cm ⁻¹	silicone band 515 cm ⁻¹	analyte band 1130 cm ⁻¹	analyte band 1081 cm ⁻¹	analyte band 1558 cm ⁻¹	analyte band 1626 cm ⁻¹
nanostructure size	500 – 700 nm “sponge-like” structure		500 – 700 nm structure		700 nm “desert- rose like” structure with many sharp edges	width: 250 nm depth: 35-80 nm length: 200-1000 nm periodicity: 400 nm	depth: 100 nm periodicity: 250 nm and 436 nm
metal	Au		Au-Ag		Ag	Au	Ag
point-to-point reproducibility	10%	16%	14%	70%	17%	9%	20% – dry m.c. 10% – wet m.c.
storage	YES		NO		YES**	YES	YES*
wavelength used for measurement	488				514	785	488
analyte molecule investigated	BY				B2	A	B2/car
price-efficient	YES				YES	YES	NO
feasible for fat- soluble analytes measurements	YES				YES	YES	YES

m.c. – measurement conditions

* if the Ag deposition is performed right before usage

** the preparation protocol can be stopped after binding of the DNA molecules. Still, in this case 75% of the preparation protocol has to be performed short before the measurement

3.2. SERS-based applications for food analytics

3.2.1. The detection and differentiation of two B vitamins in simulated and market available fortified cereal product

As introduced in the first chapter, vitamins B2 and B12 are two of the components of the B vitamin complex and, accordingly, they are often found in the same products, either as naturally occurring (*i.e.*, meat) or as a food processing addition (*i.e.*, fortified foods). Due to this, while performing food analysis it is often required that they would be both detected (and quantified) at the same time. However, due to the fact that the two are analyzed by two different methods (HPLC is used for analyzing B2 content while micro-biological assays are used for analyzing B12 content as gold standard analytical tools) the total time and price of the processes is rather high. Accordingly, developing a SERS-based approach for the simultaneously detection (and, eventually, the quantification) of the two B vitamins could, in time, lead to more time (and price) effective analysis. Still, in order to do so, the first step consisted in the spectroscopic characterization of the two vitamins.

Upon analyzing the extinction spectra of B2 and B12 (**Figure 2**) it was found that an additional gain from the resonant measurement conditions can be achieved for both molecules by applying a 488 nm laser through the SERS investigations. Apart from choosing the excitation wavelength, further consideration was given to the exact measurement conditions. First, in order to develop an analytical tool that can be applied for different food matrixes, a food extraction protocol must be applied to the initial food product. This would result in an extract solution that can be measured by applying the EBL-based substrates. Accordingly, upon an extensive literature research, existing extraction protocols (referred to as CE1 and CE2 and described in the *Materials and methods* section) were chosen. However, as these protocol results in solutions having acidic pH and do not account for the full removal of either starch, sugars or proteins, the first steps of the study consisted in the understanding of the analysts SERS fingerprint at a slightly acidic pH (pH 6), the stability of the applied substrate at this pH and

the consequence of increasing the matrixes' complexity on both the SERS fingerprint of the two vitamins and the substrate's stability.

Regarding the SERS measurement procedure, it was found that by using a drop-and-dry or incubate-and-dry protocol a rather thick layer of analyte solution is formed on the substrate, occluding the SERS measurement. Further on, by using an additional, washing step, the silver film on the substrate is reaped off due to the combined effect of the chloride interaction with the substrate during the incubation and the following mechanical handling of the substrate. Accordingly, in a first approach, however, the measurements were performed by incubating the substrates in a Petri dish containing 2.5 ml of the as-prepared solutions for 10 min and measuring them under wet conditions afterwards. Moreover, it is expected that the stability of the substrate can be increased by different, chemical and/or physical procedures such as by adding a small quantity of starch to the analyte matrix¹²⁸, by using less aggressive buffers for pH adjustments (i.e. acetate buffer), by introducing functional, protective layers or by depositing a thin, protective layer (i.e., alumina)¹⁰⁰ via atomic layer deposition – ALD). Out of these different approaches, the simple addition of starch to the analyte solution was chosen as a first test due to the fact that the targeted food product tested for the application (fortified cereal product) already contains starch in its composition.

The SERS fingerprint of B2 and B12 at a pH of 6, both the ones of the pure analytes and the ones measured in the presence of starch, are depicted in **Figure 16**. As observed, a good identification of B2 can be achieved both in the case of the pure analyte solutions and in the presence of starch. Before the addition of starch, the most intense band identified in the spectra is the relatively broad one centered around 1321 cm^{-1} (assigned to the twisting C-H vibration in the aliphatic C-H chain¹¹²) and the one centered around 1529 cm^{-1} (assigned to the convoluted contribution of the in-plane ring II, III bending vibrations¹¹²). These findings are in good agreement with the experimental measurements and theoretical calculations of M. Dendisová-Vyškovská *et al.*¹¹² according to which the B2 molecule bounds to the substrate via the heterocyclic rings II and III. The presence of starch, however, induced some changes to the band ratio in the SERS spectrum: the band centered at 1626 cm^{-1} (and assigned to the in-plane ring bending vibration of ring III as well as N–H and C=O stretching vibrations, all belonging to ring III¹¹²)

became more intense in the presence of starch; the bands centered at 1536 cm^{-1} (assigned to the in-plane ring bending vibrations of ring I as well as the asymmetric bending vibration of CH_3 ¹¹²), 1400 cm^{-1} (assigned to asymmetric vibration of CH_2 in the ribityl chain¹¹²) and 1083 cm^{-1} (assigned to the convoluted contribution of the in-plane ring III bending vibration and the bending vibration of the aliphatic C-H chain¹¹²) is better defined when starch is part of the matrix. Additionally, the bands centered at 1345 cm^{-1} (assigned to the in-plane ring bending vibrations of aromatic rings II and III¹¹²) and 1321 cm^{-1} (assigned to the twisting C-H vibration in the aliphatic C-H chain¹¹²) have different intensity ratios for the different matrixes. Further on, a low intensity band centered around 1315 cm^{-1} (and assigned to the bending vibration of CH in the ribityl chain¹¹²) can be observed in the spectra of the analyte measured in the presence of starch. Considering all this aspects, it was found that a reorientation of the B2 molecule on the Ag surface occurred upon the addition of starch. More exactly, the B2 molecules is adsorbed via the heterocyclic ring III and the vibrations of the aliphatic chain are considered to be perpendicular to the surface.¹¹²

The spectra of B12 also present changes upon addition of starch (**Figure 16**). In this case, the bands centered at 1590 cm^{-1} (assigned to the out-of-phase-stretching mode of the $\text{C}=\text{C}$ bonds located along the longer corrin axis¹²⁹), 1495 cm^{-1} (assigned to the in-phase-stretching mode of the $\text{C}=\text{C}$ bonds of the corrin ring¹²⁹) and 414 cm^{-1} (assigned to the corrin ring breathing and¹²⁹) became better defined upon the addition of starch and the intensity ratio of the bands centered at 1590 cm^{-1} and 1495 cm^{-1} interchanged. Accordingly, as in the previous case, a slight reorientation of the B12 molecule towards the Ag surface is expected to have occurred upon the addition of starch. However, B12 is a big molecule and a conclusion regarding to its exact orientation is rather challenging.

All in all, the SERS spectra depicted in **Figure 16** reveals that the presence of starch does not have any detrimental effect on the SERS measurements. Instead, for both vitamins, the same signal intensity is achieved in the presence or absence of starch. Additionally, the Raman bands become better defined upon addition of starch. This is, however, not the typical situation when increasing the matrix complexity.

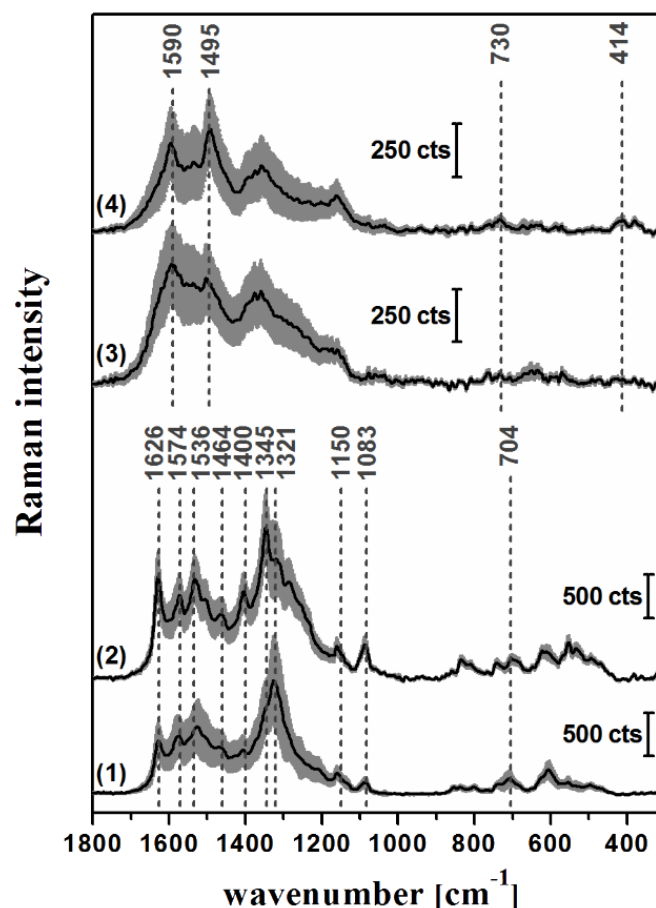


Figure 16 SERS fingerprint spectra of B2 (1) and B12 (3) at pH 6 in the as-prepared analyte solutions and SERS fingerprint spectra of B2 (2) and B12 (4) at pH 6 in the presence of starch as a stabilizing agent.

To get a better understanding of the obtained results, SEM images of the measured fields were acquired and analyzed. They are depicted in **Figure 17**. For a better understanding of the substrates stability at different pHs and due to the fact that the available literature predicts that the final pH values of the extracts are generally between 4 and 6^{30, 106, 130}. SEM images depicting the substrates stability at pH 4 and 6 are presented in **Figure 17** and discussed above. As observed, upon incubation in distilled water alone (**B**), the surface of the SERS-active substrate seems to be slightly changed, while mainly conserving the same features as the as-prepared substrate (**A**). However, upon incubation in a B2 solution of pH 6 the surface of the substrate seems to be strongly destabilized (**D**), which is visible as a displacement of the Ag layer from the substrate's surface. Same effect can be observed for the pH 4 B2 and pH 4 B12 solution incubation (**C** and **G**). However,

the effect is less dramatic. Further on, this destabilizing effect cannot be observed in the case for the B12 solution of pH 6 (**H**). While the Ag destabilizing is an expected effect caused by the usage of hydrochloric acid for pH adjustment, it was found that the presence of the B12 molecule has a beneficial effect for the Ag layer at higher pH values. A further observation was reached upon the addition of starch to the matrix: its presence has a beneficial effect regarding the stability of the Ag layer in the case of B2 for both investigated pHs (**E** – pH 4 and **F** – pH 6) and in the case of the pH 4 B12 analysis (**I**). By combining the two observations one can conclude that the Ag clustering effect caused by the hydrochloric acid can be balanced to some extent by presence of bigger molecules that act as stabilizing agents.

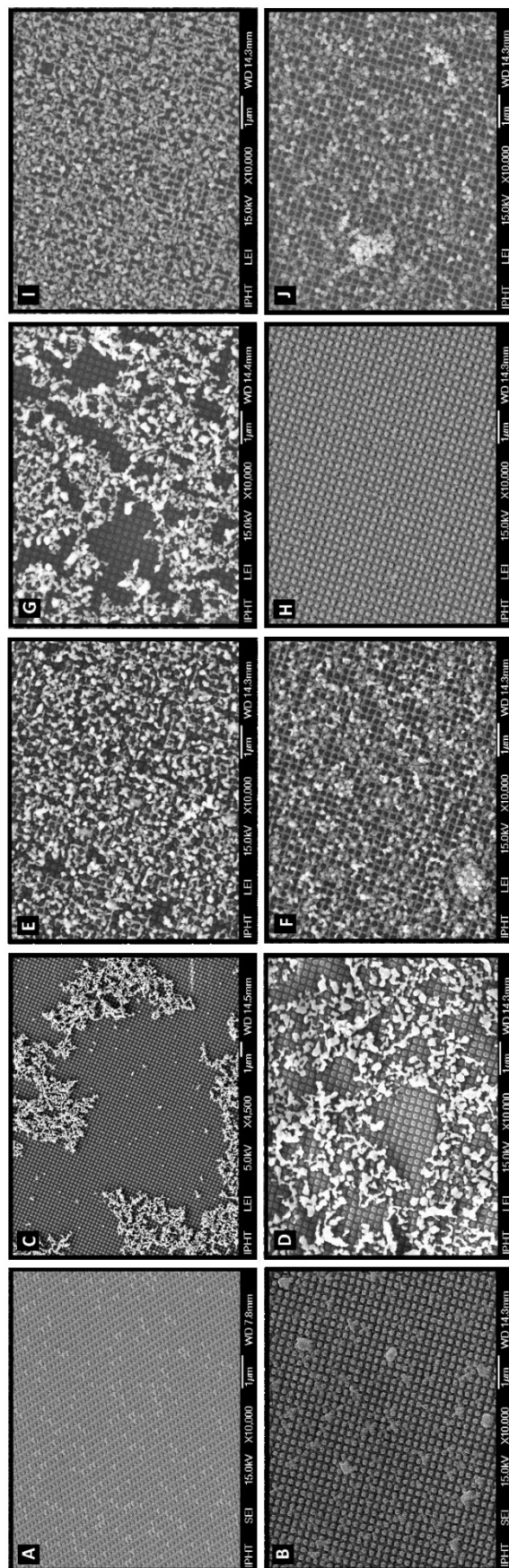


Figure 17 SEM images of the measured SERS active substrates: as-prepared substrate (A), substrate upon incubation in distilled H₂O (B), substrate upon incubation in B2 solution at 4 pH (C), substrate upon incubation in B2 solution at 6 pH (D), substrate upon incubation in B2 solution at 4 pH and in the presence of starch (E), substrate upon incubation in B2 solution at 6 pH and in the presence of starch (F), substrate upon incubation in B12 solution at 4 pH (G), substrate upon incubation in B12 solution at 6 pH (H), substrate upon incubation in B12 solution at 4 pH and in the presence of starch (I), substrate upon incubation in B12 solution at 6 pH and in the presence of starch (J).

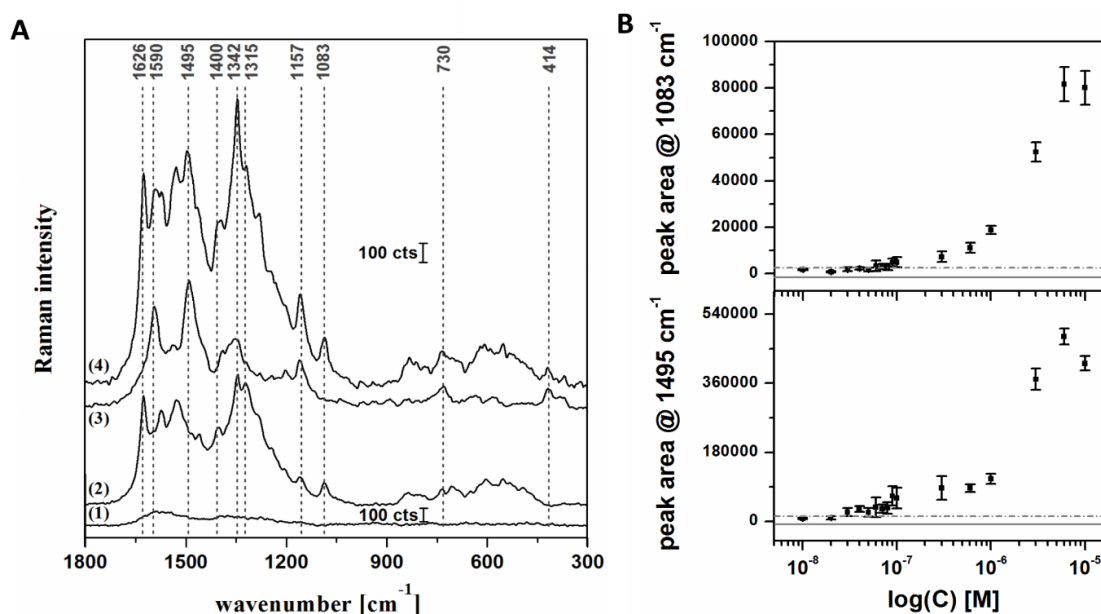


Figure 18 SERS spectra (A) of the substrate's background (1); B2 in the matrix of mixed G, F, S, starch (2); B12 in the matrix of mixed G, F, S, starch (3); B2 mixed with B12 (1:1; v/v) in the matrix of mixed G, F, S, starch (4). The integrated peak area of the Raman peak at 1083 cm⁻¹ for B2 and 1495 cm⁻¹ for B12 are also depicted (B). For all presented spectra the components concentrations are: starch (5.48 mg/ml), G (3.31 mM), F (3.31 mM), S (3.31 mM), B2 (100 nM) and B12 (100 nM). In Figure B the signal of the blank is marked by a continuous gray line and the limit of detection (equal to the signal of the blank plus three times the standard deviation of the blank) is marked as a gray dotted line.

Upon combining the information revealed by the analysis of **Figure 16** and **Figure 17** it was concluded that in the next experimental step the complexity of the matrixes would be further increased by the addition of sugars to form the BSFM.

The starting point toward defining the composition of the BSFM used in the following experiments was the information provided by the producer of the target food analyte used in this study (a market-available fortified cereal) as printed on its box and summarized in **Table 1**. However, in a first approach, only six of these components were considered for the BSFM: G, F, S, starch, B2 and B12, neglecting the lipid/protein and salt content, as well as the other vitamins present in the matrix. Further on, to decrease the viscosity of the analyte solution, the measured BSFM contained 1:9 dilutions of the values in **Table 1**, leading to

the final concentrations of the sugar/starch: 3.31 mM G, 3.31 mM F, 3.31 mM S and 5.48 mg/ml starch. Starting from this, the detection of B2 and B12 in the BSFM was first tested independently from each other and then the simultaneous detection of a 1:1 mixture of the two B vitamins in the BSFM was also tested. At this time, the concentration of the B vitamins was kept constant at 100 nM. The obtained SERS spectra are depicted in **Figure 18A**. As observed, the SERS spectrum of the mixture of G, F, S and starch (**1**), considered the background measurement, revealed no important spectral contribution from the matrix. Upon the addition of a 100 nM of B2 a clear fingerprint identification of this molecule was achieved (**2**). Moreover, by comparing these to the fingerprint of the spectra of the analyte solution measured in the presence of starch alone (**Figure 16(2)**) with the spectra measured in the presence of all the sugar/starch components (**Figure 18A(2)**) one can observe that the band centered at 1315 cm^{-1} (assigned to the bending vibration of CH in the ribityl chain)¹¹² becomes more well defined. No other relevant change can be observed to the SERS fingerprint of the analyte upon the addition of all other matrix components. As compared to this, the SERS fingerprint of B12 measured in the presence of the more complex matrix (**Figure 18A(3)**) presents better defined bands as compared to the spectra measured in the presence of starch alone (**Figure 16(4)**). Additionally, the two peaks in the region $1330\text{-}1378\text{ cm}^{-1}$ are replaced by a broad band. Considering these results, the next step consisted in the preparation of the five-component BSFM containing G, F, S, starch, B2 and B12. In a first approach, the concentrations of both B2 and B12 were 100 nM. The obtained SERS spectrum is depicted in **Figure 18A(4)** and a clear identification of both B vitamins can be achieved as proven by the presence of the bands centered at 1626 , 1400 and 1083 cm^{-1} in the case of B2 and the bands centered at 1590 , 1495 and 414 cm^{-1} in the case of B12.

Next, an estimation of the LoD for the two B vitamins in the five-component BSFM was performed by keeping the concentrations of the sugar/starch components constant and varying the concentration of the vitamins from $10\text{ }\mu\text{M}$ to 10 nM . While doing this, however, the ratio of B2:B12 was kept to 1:1. The obtained results are depicted in **Figure 18** and reveal a LoD of 70 nM for both molecules in the BSFM. According to the information provided on the cereal box, the concentration of B2 and B12 in the cereal are $3.19\text{ }\mu\text{M}$ and 1.55 nM

respectively. In the case of B2 this concentration is higher than the LoD achieved. Still, the cereal concentration of B12 is not in the detection limit of B12 in the BSFM. Regardless of this, one should keep in mind that the obtained results are only consistent with the case of an artificially prepared matrix and might not perfectly fit the analytical situation obtained during the analysis of an actual food extract (due to the different interactions of the components in the naturally occurring food products). Accordingly, in the next step two different food extraction protocols were tested for the processing of the cereal sample and the obtained solutions (**Figure 19A**) were further analyzed by both SERS and HPLC. The two tested extraction protocols (described in the *Materials and methods* section in detail) were optimized either for the extraction of B2 or B12. More exactly, the method optimized for the extraction of B2 resulted in a solution further referred to as CE1 and it required an overnight incubation, making the total extraction time quite long (approximately 20 h). As compared to this, the second protocol was applied in a much shorter time (approximately 6 h) due to no requirements of overnight incubation and resulted in a solution further referred to as CE2. As in the previous cases, during the following SERS measurements the extracts were first used in order to incubate the substrate for 10 min and then the SERS measurements were performed under wet conditions (**Figure 19B**). The obtained results are depicted in **Figure 20** and summarized in **Table 5**.

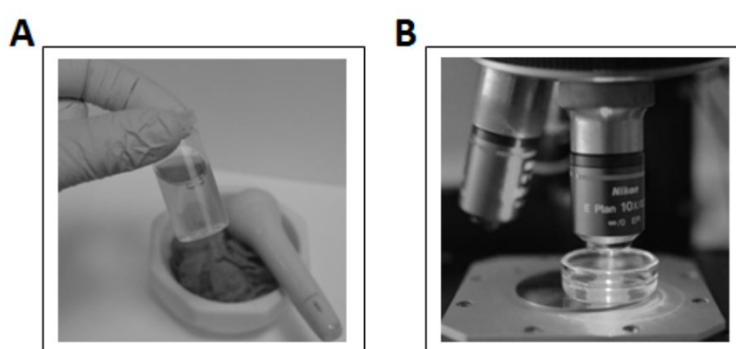


Figure 19 Schematic representation of the fortified cereal measurement protocol. The first step consisted in the preparation of the analytes to be measured by applying one of the extraction protocols described in the *Materials and methods* section (A). The resulting solutions (A) were used for incubating the SERS active substrate for 10 min and then the substrates were measured by means of SERS (B).

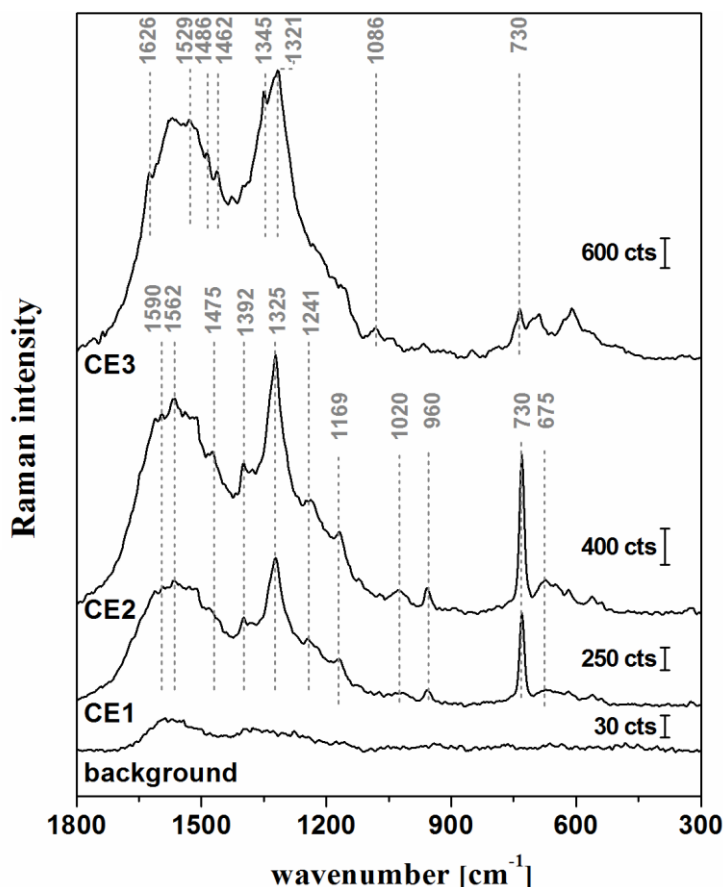


Figure 20 SERS fingerprint of the substrates background, the fortified cereal extract spectra of samples CE1, CE2 and CE3.

A close analysis of the spectra depicted in **Figure 20** and belonging to CE1 and CE2 reveals a low-intensity band centered at 1565 cm^{-1} that can be assigned to B2. Additionally, both spectra present a broad band centered at 1325 cm^{-1} and some additional low intensity bands centered at 1475 (CE2), 1392 (CE1 and CE2), 1241 (CE1 and CE2), 1169 (CE1 and CE2), 1020 (CE2), 960 (CE1 and CE2) and 675 (CE2) cm^{-1} that can be assigned to either B2 or proteins.^{112, 131, 132} Considering that the applied extraction protocols (described in the *Materials and methods* section) do not include a protein removal step and that according to **Table 1** the cereal sample includes proteins, it is expected that the investigated extracts (both CE1 and CE2) also have proteins as part of their composition. This, consequently, makes it difficult to assign the named bands to either B2 or proteins, making the usage of either of these extraction protocols for the simultaneous detection of the two B vitamins investigated rather challenging. Still, the B2 content in the two

extracts was also estimated by HPLC (see *Materials and methods* section for details related to the measurement) and it was found that sample CE1 contains 1.55 ± 0.31 mg/100 g (4.1 ± 0.82 μ M) of B2 vitamin and sample CE2 contains 1.06 ± 0.21 mg/100 g (2.8 ± 0.56 μ M). By comparing these values with the ones provided by the producer (3.19 μ M as depicted in **Table 2**) it was concluded that the two methods can both be successfully used for the extraction of the B2 vitamin. However, HPLC is not the gold standard regarding B12 analysis, so no confirmation of its extraction was obtained. Still, by comparing the accuracy of the B2 extraction by the two methods (see **Table 5**) and the time needed for performing the extraction protocols (around 20 h for CE1 and 6 h for CE2), the more time-saving one (CE2) was chosen for further optimization by performing a follow-up solid phase extraction. The details of the work procedure are described in the *Materials and methods* section and the final solution are further referred to as CE3. At this stage of the experiments the HPLC measurements were no longer considered compulsory. The obtained SERS data is, however, depicted in **Figure 20**. This spectrum presents low intensity bands centered at 1623, 1529, 1462, 1345 and 1086 cm^{-1} and assigned to B2 and a low intensity band centered at 1486 cm^{-1} and assigned to B12. Additionally, the band centered at 730 cm^{-1} and the one centered at 1325 cm^{-1} can still be detected. The latter is, most probably, due to protein residue left in the extract, while for the former can be assigned either to the proteins as well or to the B12 molecule (as it was reported by Z. Zhang et al. in the SERS spectra of B12¹³³).

Table 5 Summary of the cereal sample analysis results.

Extraction protocol	Concentration provided by the producers		Concentration as determined by HPLC		SERS detection of the vitamins	
	B2	B12	B2	B12	B2	B12
CE1	3.19 μ M	1.55 nM	4.1 ± 0.82 μ M	×	×	×
CE2	3.19 μ M	1.55 nM	2.8 ± 0.56 μ M	×	f.i.	x
CE3	3.19 μ M	1.55 nM	- *	×	f.i.	f.i.

* No HPLC measurements were performed as the work was only performed for the optimization of the SERS results.

× The technique provided no information regarding the presence of the analyte in the sample.

f.i. Fingerprint identification of the analyte in the extract.

In conclusion, the simultaneous SERS-based detection of two food relevant molecules (vitamins B2 and B12) was tested and achieved in the case of a five-component simulated food matrix (containing G, F, S, starch, B2 and B12) and a LoD of 70 nM was achieved for both vitamins. Upon this, two different food extraction protocols (optimized for the extraction of B vitamins from a higher range of food samples (i.e., beverages, dairy products, vitamin premixes or milk/soy based infant formulas)) were used for the extraction of the vitamins from a fortified cereal acquired from the area of Jena (Germany). Moreover, the less time consuming protocol from the two was further optimized toward protein removal. All samples were measured by SERS and, in the case of the optimized extraction protocol, fingerprint bands specific for both B2 and B12 could be identified.

3.2.2. The estimation of the amount of two carotenoids in tomatoes

As introduced in the first chapter, β -car and lyc are two (out of 600 known) carotenoids that can be found in the same plants. As depicted in **Figure 1**, during the maturing of the plant, the different carotenoids go through processes such as cyclization or hydroxylation and transform from one to another. Accordingly, different carotenoids can be present in the same product at the same time. Tomato fruits, for example, contain phytoene, phytofluene, β -car, ζ -car, γ -car, lyc and neurosporene in different ratios while going through the different ripening stages. Still, at the time when they are harvested and commercialized (red color phase) the main components of the tomato are β -car and lyc.^{80, 134} Moreover, it was found that just 6 of the carotenoids naturally occurring are present in the human plasma: α - and β -car, β -cryptoxanthin, lyc, lutein and zeaxanthin.^{33, 34} Due to this two reasons and due to the important functions β -car and lyc have in the human organism upon ingestion (already discussed in the first chapter) the two molecules were chosen as target analysis in this study. More exactly, it is important (for health reasons) to detect and quantify the amount of β -car (due to its pro-vitamin A activity) and lyc (due to its role toward decreasing the risk of cancer development⁴⁰) independently present in different food matrixes. In this study, four different tomato ripening

stages were chosen as targeted food for testing the potential and limitations of applying SERS for the differentiation and quantification of β -car and lyc in food. For this, however, different experimental steps were performed, and the first consisted in the understanding of the Raman fingerprint of the two carotenoids.

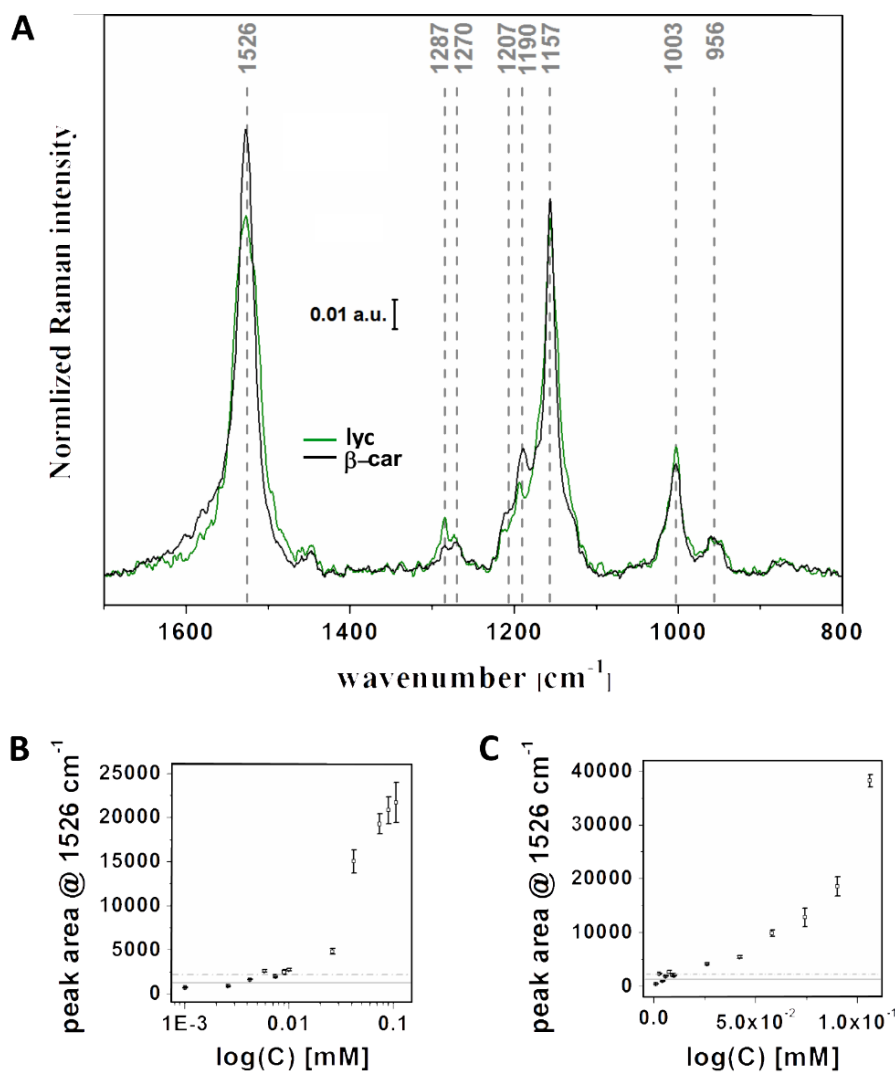


Figure 21 SERS fingerprint of lyc and β -car (A) and the integrated peak area of the Raman band centered at 1526 cm^{-1} for lyc (B) and β -car (C). In Figure B and C the signal of the blank is marked by a continuous gray line and the limit of detection (equal to the signal of the blank plus three times the standard deviation of the blank) is marked as a gray dotted line.

The SERS fingerprint of the two carotenoid molecules by applying the SERS-active substrate and a 488 nm laser for excitation (which allowed for an additional gain due to resonance measurement conditions as observed from **Figure 2**) is depicted in **Figure 21A**. Upon investigation of these spectra it can be observed that most of the bands in the fingerprint of the two molecules overlap. Still, a few differences can be identified. The band ratio of the bands centered at 1526 cm^{-1} (assigned to C=C in-phase stretching of the polyene chain of the two molecules^{122, 125}) and 1155 cm^{-1} (assigned to C-C stretching vibrations of the polyene chain of the two molecules^{122, 125}) changes when comparing the case of β -car with that of lyc. The situation is the same for the case of the two low intensity bands centered at 1270 cm^{-1} (assigned to C-H rocking vibration of the polyene chain of the two molecules¹²⁵) and 1287 cm^{-1} (assigned to ring methylene twist¹²²). Further on, the band centered at 1190 cm^{-1} (and assigned to C-C stretching vibration^{122, 125}) presents a 5 cm^{-1} shift regarding its position in the spectra of β -car and lyc (the spectral resolution provided by the experimental setup was 2 cm^{-1} as introduced in the *Materials and methods* section). Due to the existence of these differences it was expected that by combining a well-defined experimental protocol (that would result in a reliable database) with a solid analytical tool the goal of the study could be achieved. As a first step, however, an estimation of the LoD of the two carotenoids as pure analyte solution was performed and the results are depicted in **Figure 21B-C**. For this, different concentration ranging from $106\text{ }\mu\text{M}$ to $1\text{ }\mu\text{M}$ were tested and the LoD of $26\text{ }\mu\text{M}$ and $10\text{ }\mu\text{M}$ were achieved for β -car and lyc respectively.

Considering a few aspects such as the achieved LoD for the detection of β -car and lyc as pure analyte solutions, the goal of discriminating among them in a food sample and the fact that they would be present in different ratios at different ripening stages of the food product, different lyc/ β -car mixtures were prepared and measured by SERS. The individual percentages of these two analytes in each solution was decided to insure for the building of a model that would consider all intermediate stages starting with the presence of lyc alone (before the plant formation of β -car) and ending with the presence of β -car alone (upon the full transformation of lyc). The exact percentages of these two analytes in each solution (and the afferent individual concentrations) are provided in **Table 2**.

Further on, the measured SERS spectra are depicted in **Figure 22**. However, for a better visualization, the spectral range from 1030 cm^{-1} to 1330 cm^{-1} alone is depicted in **Figure 23A**. As observed here, the two low intensity bands centered at 1270 cm^{-1} and 1287 cm^{-1} gradually interchange ratios as the predominant analyte in the mixture changes from lyc to β -car. Additionally, the small bands centered at 1190 cm^{-1} and 1207 cm^{-1} becomes more defined when β -car becomes the predominant analyte.

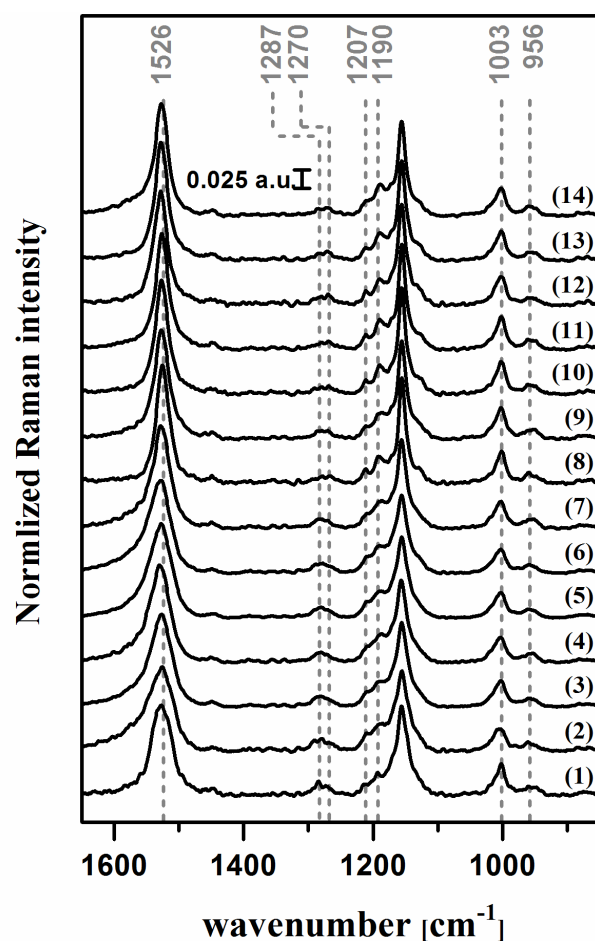


Figure 22 SERS fingerprint of the β -car/lyc mixtures in the spectral range 1330 and 1030 cm^{-1} (A), arranged based on the variation of the two analyte percentages: 0% β c and 100% lyc (1), 8% β c and 92% lyc (2), 16% β c and 84% lyc (3), 24% β c and 76% lyc (4), 32% β c and 68% lyc (5), 40% β c and 60% lyc (6), 48% β c and 52% lyc (7), 56% β c and 44% lyc (8), 64% β c and 36% lyc (9), 72% β c and 28% lyc (10), 80% β c and 20% lyc (11), 88% β c and 12% lyc (12), 96% β c and 4% lyc (13), and 100% β c and 0% lyc (14).

To build a strong analytical tool the next step consisted in performing statistical analyzes of the data by building and applying a PCA-PLSR model. This analytical tool was built by O. Ryabchykov and T.W. Bocklitz as part of a collaboration resulting in a publication¹²⁴. A detailed explanation of the analytical procedure is provided in the *Materials and methods* section. Within this analysis, a PCA^{93, 94} was performed using different number of principal components. This was followed by a PLSR^{93, 94} analysis, also using different number of components and two types of cross-validation. More exactly, for building the training data set all values representing one concentration (carotenoid percentages) were removed (and this was repeated for all different concentrations). The obtained root mean square error (RMSE) values are depicted in **Figure 23B** under the denomination SA1. In a next step, 1% of the total number of measurements was randomly taken out for training. The obtained the RMSE values are also depicted in **Figure 23B** under the denomination SA2. Finally, the optimal number of principal components for PCA and PLS were decided for, and a model was built using all of the measured data. This model was then applied for the prediction of the lycopene/ β -carotenoid percentages in food. The obtained RMSE values for the different considered PCA-PLS component numbers are depicted in **Figure 23B**.

Upon analyzing **Figure 23B** it can be observed that by using a PCA/PLS combination of more than 4 PCA components and 2 PLS components no further improvement of the RMSE is achieved, independent of the cross-validation approach used. Instead, a saturation plateau is reached and overfitting might occur. To avoid this, 4 PCA and 2 PLS components was the chosen combination for further data analysis within the study and the achieved RMSE value for data training was 11.7%. The afferent cross-validated regression results are depicted in **Figure 23C**. Considering this, it was expected that the accuracy of the proposed SERRS method in predicting the concentrations of food samples would be around the same level.

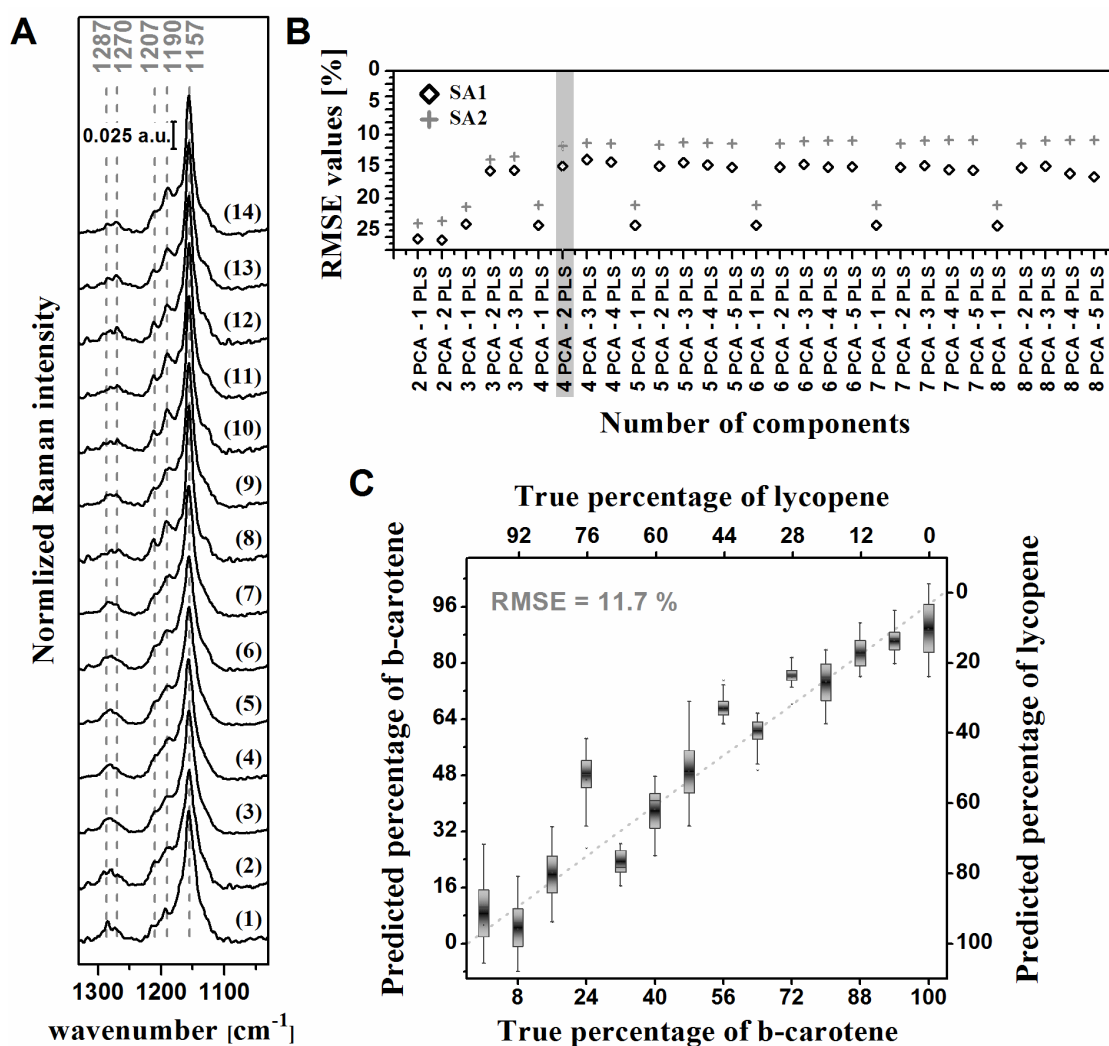


Figure 23 SERS fingerprint of the β -car/lyc mixtures in the spectral range 1330 and 1030 cm^{-1} (A), arranged based on the variation of the two analyte percentages: 0% β c and 100% lyc (1), 8% β c and 92% lyc (2), 16% β c and 84% lyc (3), 24% β c and 76% lyc (4), 32% β c and 68% lyc (5), 40% β c and 60% lyc (6), 48% β c and 52% lyc (7), 56% β c and 44% lyc (8), 64% β c and 36% lyc (9), 72% β c and 28% lyc (10), 80% β c and 20% lyc (11), 88% β c and 12% lyc (12), 96% β c and 4% lyc (13), and 100% β c and 0% lyc (14). RMSE values for various numbers of components used for PCA and for PLS (B) and cross-validation analysis results obtained for the case of the 4-component PCA and 2-component PLS analysis (C).

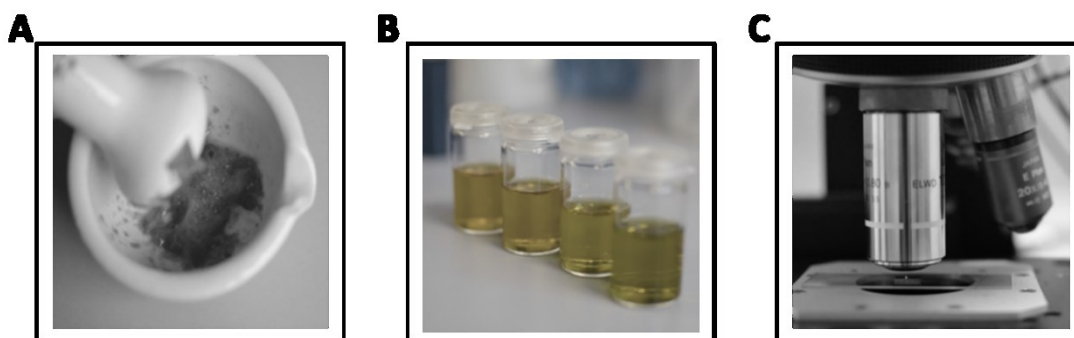


Figure 24 Schematic representation of the tomato measurement protocol. The first step consisted in the preparation of the analytes to be measured by applying the extraction protocol described in the *Materials and methods* section (A). The resulting solutions (A) were used for incubating the SERS active substrate for 30 min and then the substrates were measured by mince of SERS (B).

In the next experimental stage two different tomato series were chosen as test analytes for application of the developed analytical tool. Each tomato series contained four cherry tomatoes belonging to different ripening stages, ranging from orange to red. As mentioned before, the orange-to-red ripening stages were chosen in order to account for β -car and lyc being the main carotenoid species present in the tomatoes at the time and also to account for the “on-field” situation according to which the harvesting occurs before the tomatoes reach the final ripening stage. Instead, the red-ripening stage is often reached in the shop storage conditions. To also account for this, for the first tomato series (further referred to as G1 to G4) the tomatoes were picked from the plant upon reaching the different ripening stages while for the second tomato series (further referred to as L1 to L4) the tomatoes were picked from the plant at the same early ripening stage (yellow) and the other 3 ripening stages were achieved in simulated lab-ripening conditions. For this, the vegetables were illuminated with an 11 W lamp for the needed period of time and upon reaching a different ripening stage one tomato of the batch was frozen. They were kept at -20°C until the time when the extraction and measurement were performed. A detailed description of the extraction protocol (**Figure 24A**) is provided in the *Materials and methods* section and the resulting solutions (**Figure 23B**) were used for incubating the SERS-active substrates for 30 min before performing SERS measurements under dry conditions (**Figure 24C**). The measured SERS spectra are depicted in **Figure 25**, together with sample

pictures of the four different tomato ripening stages investigated. The SERS spectra are very similar to the ones depicted in **Figure 21**. Still, differences can be observed as the spectra in **Figure 25** are a result of a measurement of the extract containing more than one single type of carotenoid molecules which interact with each-other and with the substrate. Moreover, as mentioned before, the extract is expected to also contain other carotenoids than β -car and lyc (i.e. phytoene, phytofluene, ζ -car, γ -car and neurosporene)

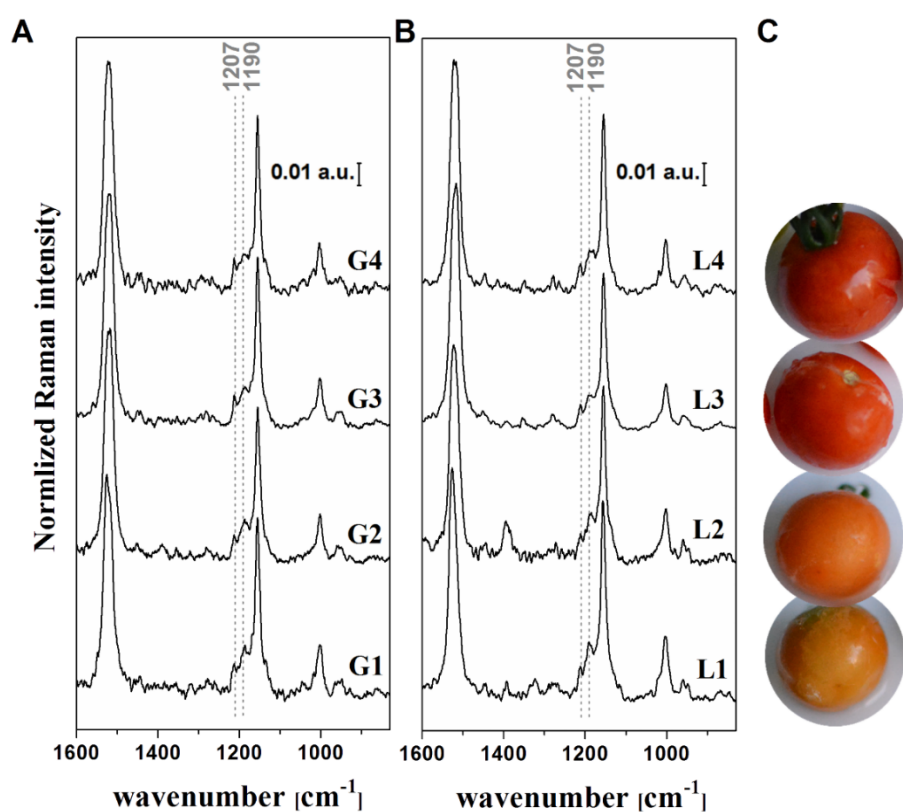


Figure 25 SERS fingerprint of the garden-ripening tomato batch (A) and the lab-ripening tomato batch (B), as well as sample pictures of the colors the tomatoes had when analyzed (C).

Table 5 Percentage of lyc and β c estimated in the tomato extracts by means of HPLC and SERS measurements.

		HPLC results				SERS results*	
		lyc	β c	lyc**	β c**	lyc	β c
		μ M	μ M	%	%	%	%
plant-ripening	G1	10.7 \pm 1.1	7.8 \pm 0.8	57.9	42.1	41.5 \pm 12.9	58.5 \pm 12.9
	G2	30.0 \pm 3.0	10.6 \pm 1.1	74.0	26.0	70.1 \pm 6.4	29.9 \pm 6.4
	G3	51.5 \pm 5.1	13.4 \pm 1.3	79.3	20.7	67.2 \pm 9.4	32.8 \pm 9.4
	G4	20.8 \pm 2.1	12.0 \pm 1.2	63.4	36.6	59.6 \pm 15.6	40.4 \pm 15.6
lab-ripening	L1	13.1 \pm 1.3	10.7 \pm 1.1	55.1	44.9	11.3 \pm 10.4	88.7 \pm 10.4
	L2	27.9 \pm 2.8	13.2 \pm 1.3	67.9	32.1	48.1 \pm 9.0	51.9 \pm 9.0
	L3	99.7 \pm 9.9	14.6 \pm 1.5	87.2	12.8	86.6 \pm 5.7	13.4 \pm 5.7
	L4	54.8 \pm 5.5	18.0 \pm 1.8	75.3	24.7	63.9 \pm 4.8	36.1 \pm 4.8

* PLS score value

** the % calculation was performed by considering that lyc and β -car are the only two carotenoids present in the extract.

The tomato SERS measurement data were statistically analyzed by applying the already discussed PCA/PLS model by applying the same pre-processing steps. The value obtained for the RMSE was 18.9%. The results (in the form of PLS scores obtained by applying the PCA-PLS regression analysis) are presented in **Table 5**. In order to confirm the SERS results, HPLC measurements were also performed on the same extracts (a detailed description is provided in the *Materials and methods* section) and the results can also be found in **Table 5**. By comparing the SERS and HPLC results a quite good agreement in between the two analytical tools was observed. The one, important exception is in the case of samples L1 and L2, where it is expected that an error occurred due to miss-assignments of other carotenoids present in the extract (i.e., phytoene, phytofluene, ζ -car, γ -car and neurosporene). The prediction accuracy should, however increase upon considering more of the carotenoids in the building of the model. Yet another possible procedure for further improving the outcome of the analytical method is by building the training dataset based on a combination of SERS spectra and HPLC measurements of tomatoes at different ripening stages. In this approach more intermediate ripening stages should be considered and for each investigated tomato both SERS spectra and HPLC measurements should be performed. Upon this, chemometric-based analysis would, ideally, result in an analytical tool that

would, ideally, be able to estimate the composition of unknown samples without using any lab-designed simulated matrix measurements, but with accounting for the different other carotenoids present in the tomatoes. This is, however, beyond the aim of this study but would be of interest in a follow-up study. Further information can be gathered from the data in **Table 5** in order to answer the initial inquiries of the study. First, it can be observed that the lyc content still increases when the fruit ripening is achieved in lab/shop conditions. This is an important fact regarding the food industry, where tomatoes go through a harvesting-delivery-shop storage time-intervals before reaching the costumers and being consumed. However, early harvesting does not seem to badly influence the quality of the tomato fruit. Second, it can be observed that upon reaching the red-ripening stage the lyc content decreases most probably in favor of other carotenoids. This information becomes relevant when deciding on a dietary regime toward a health-improving result.

In conclusion, the simultaneous SERS-based detection and quantification of two carotenoids (β -car and lyc) in cherry tomato samples was tested. In order to achieve this, a PCA/PLS model was build based on a simulated matrix containing different mixtures of β -car and lyc. The percentages in which the two carotenoids were mixed were chosen to simulate the different possible β -car/lyc compositions in tomatoes. Upon this, two different tomato series containing four different ripening stages were processed according to a protocol that can be applied for carotenoid extraction from a higher range of food samples (i.e. eggs, spinach or other vegetables). The main difference in the two tomato series consisted in the ripening procedure: tomatoes in series G reached the different stages on the plant while tomatoes on series L were picked when yellow and the different ripening stages were reached upon lab condition illumination (not on the plant). The previously constructed PCA/PLS model was applied on the data gathered upon the SERS measurements of the tomatoes and the results were compared to the HPLC measurements of the same extracts. A good agreement was obtained between the HPLC and the SERS results for most of the tomato samples.

All in all, this analytical procedure provides for a fast analysis of food samples (exemplified by the tomato series) in a fast manner. Additionally, for the case of the above introduced SERS-based approach once the full calibration

dataset is measured, the PCA-PLS analysis leading to the regression used for food sample analysis is performed at a day prior to the actual food testing and the regression result can be afterward applied at any time. In order to account for day-to-day comparison, a wavenumber calibration is performed using an external standard. Further on, by introducing an internal standard intensity calibration can eventually also be ensured for to account for all the different measurement system errors. Upon this, the SERS measurement and data analysis for one sample should not require more time than a HPLC measurement. In despite of all this advantages, HPLC remains the trusted analytical tool and work is still required in order to further develop and validate SERS for carotenoids quantification in food.

4. Summary and outlook

Within the framework of this thesis the potential and limitation of applying SERS for food analytics was assessed. To do so, different aspects had to be considered, such as (i) the choice of a substrate that would provide high and reproducible enhancement for the Raman signal of the analyte molecule; (ii) the design of a measurement procedure that would assure for a big, reliable dataset which can, ideally, be used at any later time for on-field measurements without requiring to be re-measured prior to each experiment; (iii) a good understanding of the spectral fingerprint of the different analyte molecules, which would then facilitate for the development of a strong analytical tool for reliable identification of those molecules and, eventually, also for their quantification. Apart from this, when working with naturally occurring samples (as opposed to lab-synthesized molecules) much attention is required to the understanding of the food matrix, its composition and the interactions of its different components. Moreover, when processing food samples, attention is required to the lab conditions as different food relevant analytes are unstable under normal lab illumination and air exposure (i.e. most vitamins and carotenoids). Further on, while one would expect to be able to make use of the non-invasive property of SERS, the development of applications, such as analyte quantification, requires a good understanding of the different chemical interactions of the food components. Accordingly, as a first analytical step applying a food extraction procedure is the best option. Moreover, further optimization of this procedure is often required.

As a first step of the work, different SERS-active substrates were tested to establish their analyte detection capabilities and their point-to-point reproducibility. This information, together with knowledge regarding the substrates storage capability and price-efficiency (both as cost of the technology requirements for preparation and measurement) were used in order to decide for the best-suited SERS active substrate for food analysis applications. Five different substrates were tested for this: EGNPs, Au NS, Ag/Au NS, HD-DVD and EBL-based SERS -active substrates. While all of these substrates have both advantages and disadvantages (comprehensively discussed in the *Results and discussion* part

of this thesis), by comparing all the above mentioned aspects in between all different investigated substrates, the EBL-based substrates were chosen for the actual food analysis tests. However, it is expected that a combination of the price-efficiency of the HD-DVD production and the structural precision of the tested EBL-based substrates would make for the best-suited SERS-active substrate (as far as the presented data can predict). More exactly, the EBL-based substrates were found to have a highly periodic surface that provides a high point-to-point signal detection reproducibility and can be applied for dry and wet measurements of water and fat soluble analytes. On the other hand, HD-DVD encrypting technology provides for a cost effective, rapid stamping of a predefined pit structure into a low cost material (polycarbonate). Accordingly, by imprinting the structures specific for the EBL-based substrates on the polycarbonate-like material as the one used for HD-DVD production the substrate preparation price would significantly decrease, while the homogeneity and ordered EBL-like structure would be maintained.

Regarding the food analysis, two application examples were developed and introduced within the framework of this thesis. One of them consisted in the detection of two different analytes (vitamins B2 and B12) in a fairly complex matrix (a cereal product containing no less than twelve different components: lipids, carbohydrates, fibers, proteins, salt, iron and six different B vitamins). This matrix contained relatedly high amounts of carbohydrates (82g/100g cereal) and comparably lower amounts of the two vitamins (B2: 3.19 μ M/100g cereal and B12: 1.55nM/100g cereal). The other consisted in the quantification of two different analytes (β -car and lyc) in a matrix containing five other carotenoids. Both of these applications were chosen due to the current technological challenges of their analytical methods. More exactly, B2 is analyzed by HPLC and B12 by micro biological assay as gold standard analytical tools, making the total analytical price and time not efficient. In the case of the two carotenoids the gold standard analytical tool is HPLC, but the final cost of the analysis is not cost effective. This is due to the fact that a system calibration by measuring different concentrations of the target molecules in standard solutions is required prior to each HPLC analysis and due to fact that the cost of the specific analyte molecules is high, while their shelf life is short (storage requirements: dry, dark, oxygen free space, -20°C for the

storage of crystalline β -car, -70°C for the storage of crystalline lyc and for the case of stock solutions the exact shelf life depends on the exact lab conditions and handling procedure), is also high (~ 180 euro/mg for the case of lyc and ~ 20 euro/g for the case of β -car according to Sigma Aldrich). Upon an intensive literature study and achievement of an understanding of the many differences regarding the two targeted applications, different steps were considered for the implementation of SERS and a detailed presentation of both projects is available in the *Results and discussion* part of this thesis. Briefly, as already mentioned, cereal matrixes contain high amounts of carbohydrates and the food extraction protocols do not account for their full separation from the final extract. Accordingly, as a first step of the application development an artificial matrix (containing G, F, S, starch, vitamin B2 and B12) was prepared and the LoD for the detection of the two B vitamins in this matrix was estimated. Upon this, two different extraction protocols (optimized for either the extraction of B2 or B12) were tested and the resulting extracts were measured by SERS and HPLC. Finally, one of the mentioned food extraction protocols was further optimized in order to further remove proteins and salt from the final extract and to achieve the simultaneously detection of the two vitamins. As compared to this application, in the case of the two carotenoids the targeted sample had a considerably lower amount of components. Moreover, in this case the two analytes of interest were the main components of the targeted food. As a consequence, the first step consisted in preparing and measuring a series of β -car/lyc mixtures, which were then used for building a chemometric analytical model. This model consisting in a PCA-PLSR sequence and was further applied for the analysis of two different series of tomato extracts, each of them consisting in four different cherry-tomatoes belonging to different ripening stages. The same extracts were also analyzed by HPLC and by comparing the results of the different analytical methods it was concluded that fairly good results can be achieved by using SERS and relatively simple simulated matrix. However, by increasing the number of carotenoids considered for the building of the PCA-PLSR model a further increase in the accuracy of the tomato composition prediction is expected. Nevertheless, in both tested applications (fortified cereal and tomato analysis) SERS was successful in reaching conclusions that could be also confirmed by HPLC. Considering that HPLC is a well-established technique

in food analytics and the development of SERS applications toward food analytics is still an emerging research, the reached results and conclusions present SERS as a promising analytical tool.

It is important to emphasize, however, that there are still many different aspects that need to be considered before SERS can be accepted as an alternative analytical tool to HPLC. Among these: the development of a substrate that includes an internal standard and that is chemically stable for measuring acidic (or basic) solutions; the same substrate should be easy to prepare, cost-efficient, provide a high efficiency and a high point-to-point reproducibility. Additionally, the development of an easy measurement procedure that takes into account the different requirements of working with analytes that might be unstable to normal lab conditions, as most vitamins are, and the development of an easy (computer assisted) protocol for data analysis that would allow for fast analysis are also of high importance. Most of the above mentioned requirements were carefully considered and presented through the thesis. Furthermore, considering the complexity of the food matrices and the well-known challenges of the SERS technology, the results discussed in the frame of this thesis represent a big step forward toward real life applications.

5. References

1. C. Holmberg, J. E. Chaplin, T. Hillman and C. Berg, *Appetite*, 2016, 99, 121-129.
2. M. Gallo and P. Ferranti, *Journal of Chromatography A*, 2016, 1428, 3-15.
3. L. J. Appel, T. J. Moore, E. Obarzanek, W. M. Vollmer, L. P. Svetkey, F. M. Sacks, G. A. Bray, T. M. Vogt, J. A. Cutler, M. M. Windhauser, P.-H. Lin, N. Karanja, D. Simons-Morton, M. McCullough, J. Swain, P. Steele, M. A. Evans, E. R. Miller and D. W. Harsha, *New England Journal of Medicine*, 1997, 336, 1117-1124.
4. D. W. Haslam and W. P. T. James, *The Lancet*, 366, 1197-1209.
5. B. N. Ames, *Science*, 1983, 221, 1256-1264.
6. E. F. S. Authority, <http://www.efsa.europa.eu/>.
7. U. S. F. a. D. Administration, <http://www.fda.gov/>.
8. K. Yamjala, M. S. Nainar and N. R. Ramiseti, *Food Chemistry*, 2016, 192, 813-824.
9. *Advances in Agrophysical Research*, InTech, 2013.
10. B. Hitzmann, R. Hauselmann, A. Niemoeller, D. Sangi, J. Traenkle and J. Glassey, *Biotechnology Journal*, 2015, 10, 1095-1100.
11. *Food analysis. Principles and techniques. Vol. 3. Biological techniques.*, Marcel Dekker, Inc., New York and Basel, 1985
12. J. A. Albrecht, in *NIANR, Extension - Division of the Institute of Agriculture and Natural resources at the University of Nebraska-Lincoln, Nebraska*, 2007, p. 9.
13. K. Marković, M. Hruškar and N. Vahčić, *Nutrition Research*, 2006, 26, 556-560.
14. M. Jahn, S. Patze, I. Hidi, R. Knipper, A. I. Radu, A. Muhlig, S. Yuksel, V. Peksa, K. Weber, T. Mayerhofer, D. Cialla-May and J. Popp, *Analyst*, 2015, DOI: 10.1039/c5an02057c.
15. V. Peksa, M. Jahn, L. Štolcová, V. Schulz, J. Proška, M. Procházka, K. Weber, D. Cialla-May and J. Popp, *Analytical Chemistry*, 2015, 87, 2840-2844.

16. R. A. Holley and D. Patel, *Food Microbiology*, 2005, 22, 273-292.
17. P. S. Mead, L. Slutsker, V. Dietz, L. F. McCaig, J. S. Bresee, C. Shapiro, P. M. Griffin and R. V. Tauxe, *Emerging Infectious Diseases*, 1999, 5, 607-625.
18. G. Mortensen, G. Bertelsen, B. K. Mortensen and H. Stapelfeldt, *International Dairy Journal*, 2004, 14, 85-102.
19. H. J. Powers, *The American Journal of Clinical Nutrition*, 2003, 77, 1352-1360.
20. F. Watanabe, *Experimental Biology and Medicine*, 2007, 232, 1266-1274.
21. M. Ryan-Harshman and W. Aldoori, *Canadian Family Physician*, 2008, 54, 536-541.
22. H. W. Baik and R. M. Russell, *Annual Review of Nutrition*, 1999, 19, 357-377.
23. V. Herbert, *Am J Clin Nutr*, 1988, 48, 852-858.
24. M. J. Medrano, M. J. Sierra, J. Almazán, M. T. Olalla and G. López-Abente, *American Journal of Public Health*, 2000, 90, 1636-1638.
25. K. Nilsson, S. Warkentin, B. Hultberg, R. Fäldt and L. Gustafson, *Aging Clin Exp Res*, 2000, 12, 199-207.
26. H. B. Burch, O. H. Lowry, A. M. Padilla and A. M. Combs, *Journal of Biological Chemistry*, 1956, 223, 29-45.
27. M. LANE and C. P. ALFREY, *Blood*, 1965, 25, 432-442.
28. S. A. S. Gropper, J. L. Smith and J. L. Groff, *Advanced nutrition and human metabolism*, Wadsworth/Cengage Learning, Australia; United States, 2009.
29. C. H. S. Ruxton and T. R. Kirk, *British Journal of Nutrition*, 1997, 78, 199-213.
30. E. Campos-Gimnez, P. Fontannaz, M.-J. Trisconi, T. Kilinc, C. Gimenez and P. Andrieux, *Journal of AOAC International*, 2008, 91, 786-793.
31. E. H. Harrison, C. dela Sena, A. Eroglu and M. K. Fleshman, *The American Journal of Clinical Nutrition*, 2012, 96, 1189S-1192S.
32. J. Hirschberg, *Current Opinion in Plant Biology*, 2001, 4, 210-218.
33. M. M. D. Aneta Gajowik, *Rocz Panstw Zakl Hig*, 2014, 65, 9.
34. T. Grune, G. Lietz, A. Palou, A. C. Ross, W. Stahl, G. Tang, D. Thurnham, S.-a. Yin and H. K. Biesalski, *The Journal of Nutrition*, 2010, 140, 2268S-2285S.

-
35. P. Di Mascio, S. Kaiser and H. Sies, *Archives of Biochemistry and Biophysics*, 1989, 274, 532-538.
 36. D. B. Rodriguez-Amaya, I. L. S. Institute and OMNI, *A Guide to Carotenoid Analysis in Foods*, ILSI Press, 2001.
 37. H. Bachmann, A. Desbarats, P. Pattison, M. Sedgewick, G. Riss, A. Wyss, N. Cardinault, C. Duszka, R. Goralczyk and P. Grolier, *The Journal of Nutrition*, 2002, 132, 3616-3622.
 38. J. D. Ribaya-Mercado, F. S. Solon, M. A. Solon, M. A. Cabal-Barza, C. S. Perfecto, G. Tang, J. A. A. Solon, C. R. Fjeld and R. M. Russell, *The American Journal of Clinical Nutrition*, 2000, 72, 455-465.
 39. M. Jenab, S. Salvini, C. H. van Gils, M. Brustad, S. Shakya-Shrestha, B. Buijsse, H. Verhagen, M. Touvier, C. Biessy, P. Wallstrom, K. Bouckaert, E. Lund, M. Waaseth, N. Roswall, A. M. Joensen, J. Linseisen, H. Boeing, E. Vasilopoulou, V. Dilis, S. Sieri, C. Sacerdote, P. Ferrari, J. Manjer, S. Nilsson, A. A. Welch, R. Travis, M. C. Boutron-Ruault, M. Niravong, H. B. Bueno-de-Mesquita, Y. T. van der Schouw, M. J. Tormo, A. Barricarte, E. Riboli, S. Bingham and N. Slimani, *Eur J Clin Nutr*, 0000, 63, S150-S178.
 40. J. Levy, E. Bosin, B. Feldman, Y. Giat, A. Miinster, M. Danilenko and Y. Sharoni, *Nutrition and Cancer*, 1995, 24, 257-266.
 41. P. R. H. Salvatore Fanali, Colin F. Poole, Peter Schoenmakers, David Lloyd, Elsevier, Amsterdam, 2013.
 42. M. Sulyok, R. Krska and R. Schuhmacher, *Anal Bioanal Chem*, 2007, 389, 1505-1523.
 43. L. M. L. Nollet and F. Toldra, *Food Analysis by HPLC, Third Edition*, CRC Press, 2012.
 44. M. W. Dong, *LCGC North America*, 2013, vol. 31, p. 9.
 45. S. S. Kumar, R. S. Chouhan and M. S. Thakur, *Analytical Biochemistry*, 2010, 398, 139-149.
 46. H. M. Merken and G. R. Beecher, *Journal of Agricultural and Food Chemistry*, 2000, 48, 577-599.
 47. I. M. Bird, *BMJ : British Medical Journal*, 1989, 299, 783-787.
 48. G. A. Armstrong and J. E. Hearst, *The FASEB Journal*, 1996, 10, 228-237.
 49. W. Hewitt and S. Vincent, in *Theory and Application of Microbiological Assay*, Academic Press, 1989, p. 323.
 50. H. W. Loy and W. W. Wright, *Analytical Chemistry*, 1959, 31, 971-974.

51. W. H. S. Vincent, *Academic Press, Inc.*, 1989, p. 322.
52. K. Katrin, K. Harald, I. Irving, R. D. Ramachandra and S. F. Michael, *Journal of Physics: Condensed Matter*, 2002, 14, R597.
53. P. L. Stiles, J. A. Dieringer, N. C. Shah and R. P. V. Duyne, *Annual Review of Analytical Chemistry*, 2008, 1, 601-626.
54. E. C. Le Ru, E. Blackie, M. Meyer and P. G. Etchegoin, *The Journal of Physical Chemistry C*, 2007, 111, 13794-13803.
55. U. Neugebauer, P. Rösch and J. Popp, *International Journal of Antimicrobial Agents*, 2015, 46, Supplement 1, S35-S39.
56. M. Jahn, S. Patze, I. J. Hidi, R. Knipper, A. I. Radu, A. Muhlig, S. Yuksel, V. Peksa, K. Weber, T. Mayerhofer, D. Cialla-May and J. Popp, *Analyst*, 2016, 141, 756-793.
57. D. Cialla, A. März, R. Böhme, F. Theil, K. Weber, M. Schmitt and J. Popp, *Analytical and Bioanalytical Chemistry*, 2011, 403, 27-54.
58. X.-M. Lin, Y. Cui, Y.-H. Xu, B. Ren and Z.-Q. Tian, *Analytical and Bioanalytical Chemistry*, 2009, 394, 1729-1745.
59. M. E. Stewart, C. R. Anderton, L. B. Thompson, J. Maria, S. K. Gray, J. A. Rogers and R. G. Nuzzo, *Chemical Reviews*, 2008, 108, 494-521.
60. K. A. Willets and R. P. Van Duyne, *Annual Review of Physical Chemistry*, 2007, 58, 267-297.
61. E. C. L. R. P. G. Etchegoin, *Principles of Surface-Enhanced Raman Spectroscopy*, Elsevier, 2009.
62. H. Kim, K. M. Kosuda, R. P. Van Duyne and P. C. Stair, *Chemical Society Reviews*, 2010, 39, 4820-4844.
63. D. A. Long, *The Raman Effect: A Unified Treatment of the Theory of Raman Scattering by Molecules*, Wiley, 2002.
64. X. Wei and S. Sebastian, *Reports on Progress in Physics*, 2014, 77, 116502.
65. R. Zhang, Z. Wang, C. Song, J. Yang, A. Sadaf and Y. Cui, *Journal of Fluorescence*, 2013, 23, 71-77.
66. I. J. Hidi, M. Jahn, K. Weber, D. Cialla-May and J. Popp, *Physical Chemistry Chemical Physics*, 2015, 17, 21236-21242.
67. J. F. Li, Y. F. Huang, Y. Ding, Z. L. Yang, S. B. Li, X. S. Zhou, F. R. Fan, W. Zhang, Z. Y. Zhou, Y. WuDe, B. Ren, Z. L. Wang and Z. Q. Tian, *Nature*, 2010, 464, 392-395.

-
68. H. Wang, Q. Jin, L. Yang and Y. Liu, *Journal of Nanoparticle Research*, 2013, 15, 1-9.
 69. S. Barbosa, A. Agrawal, L. Rodríguez-Lorenzo, I. Pastoriza-Santos, R. A. Alvarez-Puebla, A. Kornowski, H. Weller and L. M. Liz-Marzán, *Langmuir*, 2010, 26, 14943-14950.
 70. S. Z. Nergiz, N. Gandra, M. E. Farrell, L. Tian, P. M. Pellegrino and S. Singamaneni, *Journal of Materials Chemistry A*, 2013, 1, 6543-6549.
 71. Y. Kang, M. Si, Y. Zhu, L. Miao and G. Xu, *Spectrochim Acta A Mol Biomol Spectrosc*, 2013, 108, 177-180.
 72. R. G. Freeman, K. C. Grabar, K. J. Allison, R. M. Bright, J. A. Davis, A. P. Guthrie, M. B. Hommer, M. A. Jackson, P. C. Smith, D. G. Walter and M. J. Natan, *Science*, 1995, 267, 1629-1632.
 73. J. N. Anker, W. P. Hall, O. Lyandres, N. C. Shah, J. Zhao and R. P. Van Duyne, *Nat Mater*, 2008, 7, 442-453.
 74. X. Wang, S. Xu, H. Li, J. Tao, B. Zhao and W. Xu, *J. Raman Spectrosc.*, 2012, 43, 459-463.
 75. L. Baia, M. Baia, J. Popp and S. Astilean, *The Journal of Physical Chemistry B*, 2006, 110, 23982-23986.
 76. U. Huebner, K. Weber, D. Cialla, H. Schneidewind, M. Zeisberger, H. G. Meyer and J. Popp, *Microelectronic Engineering*, 2011, 88, 1761-1763.
 77. A. E. Grigorescu and C. W. Hagen, *Nanotechnology*, 2009, 20, 292001.
 78. F. Ren, H. Takashima, Y. Tanaka, H. Fujiwara and K. Sasaki, *Opt. Express*, 2015, 23, 21730-21740.
 79. J. D. Caldwell, O. Glembocki, F. J. Bezares, N. D. Bassim, R. W. Rendell, M. Feygelson, M. Ukaegbu, R. Kasica, L. Shirey and C. Hosten, *ACS Nano*, 2011, 5, 4046-4055.
 80. J. Qin, K. Chao and M. S. Kim, *Postharvest Biology and Technology*, 2012, 71, 21-31.
 81. T.-T. Jiang, W.-J. Shao, N.-Q. Yin, L. Liu, J.-L.-Q. Song, L.-X. Zhu and X.-L. Xu, *Chinese Physics B*, 2014, 23, 086102.
 82. T. Ding, D. O. Sigle, L. O. Herrmann, D. Wolverson and J. J. Baumberg, *ACS Applied Materials & Interfaces*, 2014, 6, 17358-17363.
 83. S. Kumar, T. W. Johnson, C. K. Wood, T. Qu, N. J. Wittenberg, L. M. Otto, J. Shaver, N. J. Long, R. H. Victora, J. B. Edel and S.-H. Oh, *ACS Applied Materials & Interfaces*, 2016, 8, 9319-9326.

-
84. M. Jahn, S. Patze, T. Bocklitz, K. Weber, D. Cialla-May and J. Popp, *Analytica Chimica Acta*, 2015, 860, 43-50.
 85. K.-M. Lee and T. J. Herrman, *Food and Bioprocess Technology*, 2016, 9, 588-603.
 86. J. Meng, S. Qin, L. Zhang and L. Yang, *Applied Surface Science*, 2016, 366, 181-186.
 87. F. Gao, Y. Hu, D. Chen, E. C. Y. Li-Chan, E. Grant and X. Lu, *Talanta*, 2015, 143, 344-352.
 88. D. Cialla, A. Marz, R. Bohme, F. Theil, K. Weber, M. Schmitt and J. Popp, *Anal. Bioanal. Chem.*, 2012, 403, 27-54.
 89. B. Sharma, R. R. Frontiera, A.-I. Henry, E. Ringe and R. P. Van Duyne, *Materials Today*, 2012, 15, 16-25.
 90. S. Schlücker, *Angewandte Chemie International Edition*, 2014, 53, 4756-4795.
 91. E. C. Le Ru and P. G. Etchegoin, in *Principles of Surface-Enhanced Raman Spectroscopy*, Elsevier, Amsterdam, 2009, DOI: <http://dx.doi.org/10.1016/B978-0-444-52779-0.00009-X>, pp. 121-183.
 92. R. M. Nix, *An Introduction to Surface Chemistry*, <http://www.chem.qmul.ac.uk/surfaces/scc/>.
 93. R. Wehrens, *Chemometrics with R. Multivariate data analysis in the natural sciences and life Sciences*, DOI: 10.1007/978-3-642-17841-2.
 94. T. Bocklitz, A. Walter, K. Hartmann, P. Rösch and J. Popp, *Analytica Chimica Acta*, 2011, 704, 47-56.
 95. C. Di Natale, A. Macagnano, F. Davide, A. D'Amico, A. Legin, Y. Vlasov, A. Rudnitskaya and B. Selezenev, *Sensors and Actuators B: Chemical*, 1997, 44, 423-428.
 96. D. Melucci, A. Bendini, F. Tesini, S. Barbieri, A. Zappi, S. Vichi, L. Conte and T. Gallina Toschi, *Food Chemistry*, 2016, 204, 263-273.
 97. X. Guo, F. Huang, H. Zhang, C. Zhang, H. Hu and W. Chen, *Meat Science*, 2016, 117, 182-186.
 98. E. Borràs, J. Ferré, R. Boqué, M. Mestres, L. Aceña, A. Calvo and O. Busto, *Food Chemistry*, 2016, 203, 314-322.
 99. O. Jović, T. Smolić, I. Primožič and T. Hrenar, *Analytical Chemistry*, 2016, 88, 4516-4524.

-
100. S. Yüksel, M. Ziegler, S. Goerke, U. Hübner, K. Pollok, F. Langenhorst, K. Weber, D. Cialla-May and J. Popp, *The Journal of Physical Chemistry C*, 2015, 119, 13791-13798.
 101. D. Wang, R. Ji, A. Albrecht and P. Schaaf, *Beilstein J Nanotechnol*, 2012, 3, 651-657.
 102. C. Vidal, D. Wang, P. Schaaf, C. Hrelescu and T. A. Klar, *ACS Photonics*, 2015, 2, 1436-1442.
 103. K. K. Hering, R. Möller, W. Fritzsche and J. Popp, *Chemphyschem*, 2008, 9, 867-872.
 104. U. Huebner, M. Falkner, U. D. Zeitner, M. Banasch, K. Dietrich and E.-B. Kley, 2014.
 105. A. Szterk, M. Roszko, K. Malek, M. Czerwonka and B. Waszkiewicz-Robak, *Meat Science*, 2012, 91, 408-413.
 106. P. Wimalasiri and R. B. H. Wills, *Journal of Chromatography A*, 1985, 318, 412-416.
 107. R. C. Team, *R: A language and environment for statistical computing*. R Foundation for Statistical Computing, Vienna, Austria, 2014.
 108. M. Omer, H. Negm, R. Kinjo, Y.-W. Choi, K. Yoshida, T. Konstantin, M. Shibata, K. Shimahashi, H. Imon, H. Zen, T. Hori, T. Kii, K. Masuda and H. Ohgaki, in *Zero-Carbon Energy Kyoto 2012*, ed. T. Yao, Springer Japan, 2013, DOI: 10.1007/978-4-431-54264-3_27, ch. 27, pp. 245-252.
 109. K. Atkinson, *An Introduction to Numerical Analysis*, Wiley.
 110. C. Wang, C. J. Berg, C.-C. Hsu, B. A. Merrill and M. J. Tauber, *The Journal of Physical Chemistry B*, 2012, 116, 10617-10630.
 111. V. R. Salares, N. M. Young, P. R. Carey and H. J. Bernstein, *Journal of Raman Spectroscopy*, 1977, 6, 282-288.
 112. M. Dendisová-Vyškovská, A. Kokaislová, M. Ončák and P. Matějka, *Journal of Molecular Structure*, 2013, 1038, 19-28.
 113. Y. Yan, A. I. Radu, W. Rao, G. Chen, K. Weber, D. Wang, D. Cialla-May, J. Popp and P. Schaaf, unpublished work.
 114. T. Uno, B.-K. Kim, Y. Saito and K. Machida, *Spectrochimica Acta Part A: Molecular Spectroscopy*, 1976, 32, 1179-1183.
 115. Z. L. Zhang, Y. F. Yin, J. W. Jiang and Y. J. Mo, *Journal of Molecular Structure*, 2009, 920, 297-300.

-
116. E. C. Le Ru, S. A. Meyer, C. Artur, P. G. Etchegoin, J. Grand, P. Lang and F. Maurel, *Chemical Communications*, 2011, 47, 3903-3905.
 117. N. R. Cioffi, Mahendra, *Nano-Antimicrobials: Progress and Prospects*, Springer Verlag, 2012.
 118. T. D. Milster, *Opt. Photon. News*, 2005, 16, 28-33.
 119. A. I. Radu, Y. Y. Ussembayev, M. Jahn, U. S. Schubert, K. Weber, D. Cialla-May, S. Hoepfner, A. Heisterkamp and J. Popp, *RSC Advances*, 2016, 6, 44163-44169.
 120. D. Gill, M. E. Heyde and L. Rimai, *Journal of the American Chemical Society*, 1971, 93, 6288-6289.
 121. D. Manor, R. Callender and N. Noy, *European Journal of Biochemistry*, 1993, 213, 413-418.
 122. N. Tschirner, M. Schenderlein, K. Brose, E. Schlodder, M. A. Mroginski, C. Thomsen and P. Hildebrandt, *Physical Chemistry Chemical Physics*, 2009, 11, 11471-11478.
 123. H. Schneidewind, K. Weber, M. Zeisberger, U. Hübner, A. Dellith, D. Cialla-May, R. Mattheis and J. Popp, *Nanotechnology*, 2014, 25, 445203.
 124. A. I. Radu, O. Ryabchykov, T. Bocklitz, U. Hubner, K. Weber, D. Cialla-May and J. Popp, *Analyst*, 2016, DOI: 10.1039/c6an00390g.
 125. M. R. López-Ramírez, S. Sanchez-Cortes, M. Pérez-Méndez and G. Blanch, *Journal of Raman Spectroscopy*, 2010, 41, 1170-1177.
 126. S. s. f. I. Optics, <https://integratedoptics.com/products/sers-substrates>.
 127. S. s. f. Silmeco, <http://www.silmeco.com/>.
 128. V. K. Sharma, K. M. Siskova, R. Zboril and J. L. Gardea-Torresdey, *Advances in Colloid and Interface Science*, 2014, 204, 15-34.
 129. T. Andruniow, M. Z. Zgierski and P. M. Kozlowski, *The Journal of Physical Chemistry A*, 2002, 106, 1365-1373.
 130. S. Ndaw, M. Bergaentzlé, D. Aoudé-Werner and C. Hasselmann, *Food Chemistry*, 2000, 71, 129-138.
 131. C.-H. Chuang and Y.-T. Chen, *Journal of Raman Spectroscopy*, 2009, 40, 150-156.
 132. A. Kandakkathara, I. Utkin and R. Fedosejevs, *Applied Spectroscopy*, 2011, 65, 507-513.
 133. Z. Zhang, B. Wang, Y. Yin and Y. Mo, *Journal of Molecular Structure*, 2009, 927, 88-90.

134. *F. Khachik, L. Carvalho, P. S. Bernstein, G. J. Muir, D.-Y. Zhao and N. B. Katz, Experimental Biology and Medicine, 2002, 227, 845-851.*

Curriculum vitae

Name Radu Andreea – Ioana
Date of birth 6.02.1987
Place of birth Turda, Romania

Education

Since 11/2012 Doctoral student at the Faculty of Chemistry and Geology, Friedrich-Schiller University, Jena, Germany
- science-scholarship - ProChance 2015, Promotion of the scientific interaction of young female researchers

10/2010 - 07/2012 M.Sc. Science and Technology of Advanced Materials at the Faculty of Physics, Babeş-Bolyai University, Cluj-Napoca, Romania
- grade: 9,75 (out of maximum 10)
- ERASMUS training at the Faculty of Chemistry and Geology, Friedrich-Schiller University, Jena (11/2011 - 04/2012)
- science-scholarship at the Faculty of Physics, Babeş-Bolyai University, Cluj-Napoca (10/2011 – 07/2012)

10/2006 - 07/2010 Bachelor of Engineering at the Faculty of Physics, Babeş-Bolyai University, Cluj-Napoca, Romania
- grade: 9,93 (out of maximum 10)

Scientific results

Publications

A.I. Radu, O. Ryabchykov, T.W. Bocklitz, U. Huebner, K. Weber, D. Cialla-May, J. Popp, *Toward food analytics: fast estimation of lyc and β -car content in tomatoes based on surface enhanced Raman spectroscopy (SERS)*, *Analyst*, 141, 4447-4455, 2016.

A.I. Radu, Y.Ye. Ussembayev, M. Jahn, U.S. Schubert, K. Weber, D. Cialla-May, S. Hoepfener, A. Heisterkamp, J. Popp, *HD DVD substrates for Surface Enhanced Raman Spectroscopy Analysis: Fabrication, Theoretical Predictions and Practical Performance*, RSC Advances, 6, 44163-44169, 2016.

M. Jahn, S. Patze, I. Hidi, R. Knipper, A.I. Radu, A. Mühlig, S. Yüksel, V. Peksa, K. Weber, T. Mayerhöfer, D. Cialla-May, J. Popp, *Plasmonic nanostructures for surface enhanced spectroscopic methods*, Analyst, 141, 756-793, 2016.

A.I. Radu, M. Thum, U. Huebner, K. Weber, D. Cialla-May, J. Popp, *Toward using surface enhanced Raman spectroscopy (SERS) for food analytics: detection of vitamins B₂ and B₁₂ in simulated and food matrix extracts*, Talanta, 160, 289–297, 2016.

Y. Yan, A.I. Radu, W. Rao, H. Wang, G. Chen, K. Weber, D. Wang, D. Cialla-May, J. Popp, P. Schaaf, *Mesoscopically Bi-continuous Ag–Au Hybrid Nanosponges with Tunable Plasmon Resonances as Bottom-Up Substrates for Surface Enhanced Raman Spectroscopy*, Chemistry of Materials, 2016, DOI: 10.1021/acs.chemmater.6b02637

Conferences

A. Radu, M. Jahn, K. Weber, D. Cialla-May, J. Popp, *Application of template based plasmonic substrates in food analysis*, DoKDoK 2015, Eisenach, Germany, October 1-15, 2015. Poster

A. Radu, M. Jahn, U. Huebner, D. Cialla-May, K. Weber, J. Popp, *Differentiation of carotenoids by surface enhanced Raman spectroscopy (SERS)*, 8th International Conference on Advanced Vibrational Spectroscopy (ICAVS-8), Vienna, Austria, July 12-17, 2015. Poster

A. Radu, M. Jahn, K. Weber, D. Cialla-May, J. Popp, *Application of plasmonic nanostructures in food analysis*, Molecular Plasmonics, Jena, Germany, May 7-9, 2015. Poster

D. Cialla-May, M. Jahn, A. Radu, S. Patze, K. Weber, J. Popp, *Strategies for determining food purity and quality by using SERS as analytical tool*, SPIE Photonics Europe, Brussels, Belgium, April 14-17, 2014. Poster

A. Radu, Y. Ussembayev, S. Höppener, A. Heisterkamp, U. Schubert, K. Weber, D. Cialla-May, J. Popp, *HD DVD based substrates for SERS and their application for detecting food related analytes*, The Great Scientific Exchange (SciX 2014), Reno, Nevada, USA, September 29-October 4, 2014. Poster

A. Radu, Y. Ussembayev, D. Cialla, K. Weber, S. Höppener, A. Heisterkamp, U. Schubert, J. Popp, *Determination of vitamin A by surface enhanced Raman spectroscopy (SERS)*, 24th International Conference on Raman Spectroscopy (ICORS 2014), Jena, Germany, August 10-15, 2014. Poster

A. Radu, D. Cialla, C. Matthäus, K. Weber, J. Popp, *Characterization of vitamins by using a SERS-based detection scheme*, 7th International Conference on Advanced Vibrational Spectroscopy (ICAVS-7), Kobe Convention Center, Japan, August 25-30, 2013. Poster

A. Radu, D. Cialla, K. Weber, J. Popp, *Determination of vitamins by surface enhanced Raman spectroscopy (SERS)*, DoKDoK 2013, Suhl, Germany, October 10-11, 2013. Poster

A. Radu, D. Cialla, K. Weber, J. Popp, *Characterization of vitamins by surface enhanced Raman spectroscopy (SERS)*, Trends in Bioanalytical Imaging - Analytics and Applications, Dechema-Haus, Frankfurt am Main, Germany, May 27-28, 2013. Poster

Workshops

WITec workshop series, Dresden, Germany, one day (2013)

Scientific presentations, Friedrich-Schiller-University Jena, Germany, one day (2014)

Leadership skills, Friedrich-Schiller-University Jena, Germany, two days (2014)

Time management, Friedrich-Schiller-University Jena, Germany, one day (2014)

Speech and vocal training, Friedrich-Schiller-University Jena, Germany, one day (2014)

Acknowledgment

This part is dedicated to all, who made this interdisciplinary work possible.

I would like to start by thanking Prof. Jürgen Popp for the opportunity to work in the research group, his trust, supervision and constructive discussions.

Many thanks go to Dana Cialla-May and Karina Weber for the intensive supervision, many constructive discussions, creative ideas, giving me the opportunity to take part in many different projects, helping me improve my presentation skills and all skills related to research work.

I would like to thank the many people that developed SERS-active substrates and gave me the opportunity of working with them for testing and improving the substrates. Among them, Yera Y. Ussembayev is gratefully acknowledged for his help, work and ideas regarding the HD-DVD project. Uwe Huebner, Katrin Pippardt and Birger Steinbach (IPHT Jena) are gratefully acknowledged for their help with the EBL-based substrate fabrication and SEM measurements. Dong Wang (TU Ilmenau) is gratefully acknowledged for his help with the NSs substrates fabrication and SEM measurements. Andrea Dellith is gratefully acknowledged for her help with SEM measurements.

I am deeply grateful to Martin Jahn, Oleg Ryabchykov and Thomas W. Bocklitz for their help and support with the statistical data analyzing.

My thank you go toward the people from Food GmbH (Jena, Germany) who allowed me to work in their labs, helped with the food extraction protocols and performed the HPLC measurements: Bernd Giese, Tobias Voigt and Dr. Bianca Braha.

I am deeply grateful to my students for their help and nice collaborations: Yera Y. Ussembayev and Maria Kuellmer.

I thank Sabine Schmidt, Torsten May, Philipp Lucas and Izabella Hidi for providing the different cherry tomato batches used throughout the experiments.

I would like to also thank my friends and colleagues for a very nice and constructive work environment: Izabella Hidi, Martin Jahn, Sezin Yüksel, Richard Knipper, Sabine Schmidt, Sophie Patze, and Vera Dugandzic.

Last, but not least, I would like to thank my parents, my family, and very close friends for their unconditional, unlimited support, optimism and trust. I would like to use this space to say special thanks to Izabella Hidi, Martin Jahn, Philipp Lucas and Clara Stiebing.

Declaration of Originality

I certify that the work presented here is, to the best of my knowledge and belief, original and the result of my own investigations, except as acknowledged, and has not been submitted, either in part or whole, for a degree at this or any other university.

Ich erkläre, dass ich die vorliegende Arbeit selbständig und unter Verwendung der angegebenen Hilfsmittel, persönlichen Mitteilungen und Quellen angefertigt habe.

Jena, 31 June 2016